Nonlinear chaotic lattice field theory

X Wang, S V Williams, M N Gudorf, H Liang, and P Cvitanović

School of Physics, Georgia Institute of Technology, Atlanta, GA 30332-0430, USA

E-mail: `predrag.cvitanovic@physics.gatech.edu`

26 November 2024

Abstract. Motivated by [...]

PACS numbers: 02.20.-a, 05.45.-a, 05.45.Jn, 47.27.ed

Keywords: chaotic field theory, many-particle systems, coupled map lattices, periodic orbits, symbolic dynamics, cat maps

Submitted to: *J. Phys. A: Math. Theor.*

1. Introduction

[2023-06-26 Predrag] Tigers' version of `intro.tex`

"Amazing! I did not understand a single word!"

And indeed, there is a problem of understanding what is 'chaos' [...]

We need to motivate looking at classical ϕ^k theories, I know that there is a big push for ϕ^4 in quantum field theory, so that is likely the best way to go.

2. Deterministic lattice field theory

[2023-06-26 Predrag] Tigers' version of `FT.tex`

A scalar field $\phi(x)$ over d Euclidean coordinates can be discretized by replacing the continuous space by a d-dimensional hypercubic integer lattice $\mathbb{Z}^d$, with lattice spacing a, and evaluating the field only on the lattice points [160, 164]

$$\phi_z = \phi(x)\,, \qquad x = az = \text{lattice point}\,, \quad z \in \mathbb{Z}^d\,. \tag{1}$$

A *field configuration* (here in one spatiotemporal dimension)

$$\Phi = \cdots \phi_{-3}\phi_{-2}\,\phi_{-1}\,\phi_0\,\phi_1\phi_2\phi_3\phi_4\cdots\,, \tag{2}$$

takes any set of values in system's ∞-dimensional *state space* $\phi_z \in \mathbb{R}$. A *periodic field configuration* satisfies

$$\Phi_{z+R} = \Phi_z \tag{3}$$

for any discrete translation $R \in \mathcal{L}_{\mathbf{a}}$ in the *Bravais lattice*

$$\mathcal{L}_{\mathbf{a}} = \left\{ \sum_{i=1}^{d} n_i \mathbf{a}_i \mid n_i \in \mathbb{Z} \right\} \;=\; \left\{ \mathbf{n}\,\mathbf{A} \,|\, \mathbf{n} \in \mathbb{Z}^d \right\} \tag{4}$$

where the matrix $\mathbf{A}$ whose columns are d independent integer lattice vectors $\mathbf{a}_j$

$$\mathbf{A} = [\mathbf{a}_1, \cdots, \mathbf{a}_d] \in \mathbb{R}^{d\times d} \tag{5}$$

defines a *Bravais cell* basis.

The volume of (i.e., the number of lattice sites within) $\mathcal{L}_{\mathbf{a}}$ is defined by the volume of the parallelepiped spanned by the Bravais cell basis

$$N_{\mathbf{a}} \equiv |\det \mathbf{A}|\,. \tag{6}$$

does this need a citation? Perhaps a call to Hill? For example, the periodic orbit for the 1D ϕ^3, $\overline{101}$, reoccurs for the discrete translation $R = 3$ and this is the only (one dimensional) vector in $\mathcal{L}_{\mathbf{a}}$ so we get the obvious answer that $N_{\mathbf{a}} = 3$ i.e. there are three points in the Bravais cell of this orbit.

The action in (**??**) is given as Bravais cell sum over the Lagrangian density should the z here perhaps be a vector to signify the possibility of spatiotemporality?

$$S_{\mathbf{a}}[\Phi] = \sum_z^{\mathbf{a}} \left\{ \frac{1}{2} \sum_{\mu=1}^{d} (\partial_\mu \phi)_z^2 + V(\phi_z) \right\}\,, \tag{7}$$

The variational extremum condition (8)

$$F[\Phi_c]_z = \frac{\delta S[\Phi_c]}{\delta \phi_z} = 0\,, \tag{8}$$

yields the Euler–Lagrange equations of ϕ^k theory (27) on a d-dimensional hypercubic lattice, with *periodic state* Φ_c a global deterministic (or 'classical') solution satisfying this local extremal condition on every lattice site z.

Here, and in papers I and II [55, 137] we investigate spatiotemporally chaotic lattice field theories using as illustrative examples the d-dimensional hypercubic lattice (1) discretized Klein-Gordon free-field theory, spatiotemporal cat, spatiotemporal ϕ^3 theory, and spatiotemporal ϕ^4 theory, defined respectively by Euler–Lagrange equations (8)

$$-\Box\,\phi_z \;+\; \mu^2\phi_z \qquad\qquad = 0\,, \qquad \phi_z \in \mathbb{R}\,, \tag{9}$$
$$-\Box\,\phi_z \;+\; \mu^2\phi_z - m_z \quad = 0\,, \qquad \phi_z \in [0,1) \tag{10}$$
$$-\Box\,\phi_z \;+\; \mu^2\,(1/4 - \phi_z^2) = 0\,, \tag{11}$$
$$-\Box\,\phi_z \;+\; \mu^2(\phi_z - \,\phi_z^3) \;\;= 0\,. \tag{12}$$

For free-field theory the sole parameter μ^2 is known as the Klein-Gordon (or Yukawa) mass. The anti-integrable form [12, 13, 196] of the spatiotemporal ϕ^3 (11) and spatiotemporal ϕ^4 (12) Euler–Lagrange equations, and a rescaling away of other 'coupling' parameters, is explained below, in sections **??** and **??**.

Each periodic state is a distinct deterministic solution Φ_c to the discretized Euler–Lagrange equations (8), so its probability density is a $N_{\mathcal{L}}$-dimensional Dirac delta function (that's what we mean by the system being *deterministic*), a delta function per site ensuring that Euler–Lagrange equation (8) is satisfied everywhere, with probability

$$P_c = \frac{1}{Z} \int_{\mathcal{M}_c} d\Phi \, \delta(F[\Phi]) \,, \qquad \Phi_c \in \mathcal{M}_c \,, \tag{13}$$

where $\mathcal{M}_c$ is an open neighborhood, sufficiently small that it contains only the single periodic state Φ_c.

In [137] we verify that this definition agrees with the forward-in-time Perron-Frobenius probability density evolution [54]. However, we find field-theoretical formulation vastly preferable to the forward-in-time formulation, especially when it comes to higher spatiotemporal dimensions [55].

n-point correlation functions or 'Green functions' [185]

$$\langle \phi_i \phi_j \cdots \phi_\ell \rangle = \frac{1}{Z[0]} \int D\phi \, \mathrm{e}^{-S[\phi]} \phi_i \phi_j \cdots \phi_\ell \,. \tag{14}$$

The deterministic field theory partition sum has support only on lattice field values that are solutions to the Euler–Lagrange equations (8), and the partition function (**??**) is now a sum over configuration state space (2) *points*, what in theory of dynamical systems is called the 'deterministic trace formula' [53],

$$Z[0] = \sum_c P_c = \sum_p \sum_{r=1}^{\infty} P_{p^r} \,, \qquad P_c = \frac{1}{|\mathrm{Det}\, \mathcal{J}_c|} \,, \tag{15}$$

and we refer to the $[N_{\mathcal{L}} \times N_{\mathcal{L}}]$ matrix of second derivatives

$$(\mathcal{J}_c)_{z'z} = \frac{\delta F_{z'}[\Phi_c]}{\delta \phi_z} = S[\Phi_c]_{z'z} \tag{16}$$

as the *orbit Jacobian matrix*, and to its determinant $\mathrm{Det}\, \mathcal{J}_c$ as the *Hill determinant*. Support being on state space *points* means that we do not need to worry about potentials being even or odd (thus unbounded), or the system being energy conserving or dissipative, as long as its nonwandering periodic states Φ_c set is bounded in state space. In what follows, we shall deal only with deterministic field theory and mostly omit the subscript 'c' in Φ_c.

[2024.11.25 Xuanqi] I am writing up the results for spectrum of Jacobian, and I will add to this section when I finish.

3. Orbit stability

Solutions of a nonlinear field theory are in general not translation invariant, so the orbit Jacobian matrix (16) (or the 'discrete Schrödinger operator' [30, 191])

$$\mathcal{J}_c = \begin{pmatrix} s_0 & -1 & 0 & 0 & \cdots & 0 & -1 \\ -1 & s_1 & -1 & 0 & \cdots & 0 & 0 \\ 0 & -1 & s_2 & -1 & \cdots & 0 & 0 \\ \vdots & \vdots & \vdots & \vdots & \ddots & \vdots & \vdots \\ 0 & 0 & 0 & 0 & \cdots & s_{n-2} & -1 \\ -1 & 0 & 0 & 0 & \cdots & -1 & s_{n-1} \end{pmatrix} \tag{17}$$

is not a circulant matrix: each periodic state Φ_c has its own orbit Jacobian matrix $\mathcal{J}_c = \mathcal{J}[\Phi_c]$, with the 'stretching factor' $s_t = V''(\phi_t) + 2$ at the lattice site t a function of the site field ϕ_t.

The orbit Jacobian matrix of a period-(mn) periodic state Φ, which is a m-th *repeat* of a period-n prime periodic state Φ_p, has a tri-diagonal block circulant matrix form that follows by inspection from (17):

$$\mathcal{J}_{p^r} = \begin{pmatrix} \mathbf{s}_p & -\mathbf{r} & & & -\mathbf{r}^\top \\ -\mathbf{r}^\top & \mathbf{s}_p & -\mathbf{r} & & \\ & \ddots & \ddots & \ddots & \\ & & -\mathbf{r}^\top & \mathbf{s}_p & -\mathbf{r} \\ -\mathbf{r} & & & -\mathbf{r}^\top & \mathbf{s}_p \end{pmatrix}, \tag{18}$$

where block matrix $\mathbf{s}_p$ is a $[n\times n]$ symmetric Toeplitz matrix

$$\mathbf{s}_p = \begin{pmatrix} s_0 & -1 & & & 0 \\ -1 & s_1 & -1 & & \\ & \ddots & \ddots & \ddots & \\ & & -1 & s_{n-2} & -1 \\ 0 & & & -1 & s_{n-1} \end{pmatrix}, \quad \mathbf{r} = \begin{pmatrix} 0 & \cdots & 0 \\ & & \\ & \ddots & \vdots \\ & & \\ 1 & & 0 \end{pmatrix}, \tag{19}$$

and $\mathbf{r}$ and its transpose enforce the periodic bc's. This period-(mn) periodic state Φ orbit Jacobian matrix is as translation-invariant as the temporal cat, but now under Bravais lattice translations by multiples of n. One can visualize this periodic state as a tiling of the integer lattice $\mathbb{Z}$ by a generic periodic state field decorating a tile of length n. The orbit Jacobian matrix $\mathcal{J}$ is now a block circulant matrix which can be brought into a block diagonal form by a unitary transformation, with a repeating $[n\times n]$ block along the diagonal.

4. Observables

2022-01-19, 2023-02-11 Predrag Because of the dependence of the orbit Jacobian matrix (18) on the primitive cell $\mathbf{A}$ repeat number r, we have to distinguish the partition function $Z_{\mathbf{A}}$ defined over the finite lattice volume $N_{\mathcal{L}} = N_{\mathbf{A}}$ primitive cell from the (infinite) lattice partition function $Z_{\mathcal{L}}$, which is the sum over all distinct primitive cells.

A field configuration Φ over a primitive cell $\mathbf{A}$ of lattice $\mathcal{L}$ occurs with probability density

$$P_{\mathbf{A}}[\Phi] \,=\, \frac{1}{Z}\,\mathrm{e}^{-S_{\mathbf{A}}[\Phi]}\,, \qquad Z = Z_{\mathcal{L}}[0]\,. \tag{20}$$

Here $Z_{\mathcal{L}}$ is a normalization factor, given by the *partition sum*, the sum (in continuum, the integral) over probabilities of all configurations,

$$Z_{\mathcal{L}}[\mathsf{J}] \,=\, e^{N_{\mathcal{L}} W_{\mathcal{L}}} \,=\, \int_{\mathcal{L}} d\Phi\, P[\Phi]\, e^{\Phi\cdot\mathsf{J}}\,, \qquad d\Phi = \prod_z^{\mathcal{L}} d\phi_z\,, \tag{21}$$

where $\mathsf{J} = \{j_z\}$ is an external source j_z that one can vary site by site, and $S[\Phi]$ is the action that defines the theory (discussed in more detail in section **??**). The dimension of the partition function integral equals the number of lattice sites $N_{\mathcal{L}}$, i.e., the lattice volume (6).

Birkhoff sum [130] over primitive cell c

$$A_c = \sum_{z\in c} a_z\,. \tag{22}$$

Birkhoff average over primitive cell c

$$\langle a\rangle_c = \frac{A_c}{N_c}\,. \tag{23}$$

The free energy (the large-deviation potential?)

$$\begin{aligned} Z_{\mathbf{A}}[0] \;&=\; \sum_c e^{N_{\mathcal{L}} W_c[0]} \\ e^{N_{\mathcal{L}} W_c[0]} \,&=\, \int_{\mathcal{M}_c} d\Phi\,\delta(F[\Phi]) \,=\, \frac{1}{|\mathrm{Det}\,\mathcal{J}_c|} \end{aligned} \tag{24}$$

was originally snuck into (15) (see (**??**), (**??**), (**??**)) See also partition function (**??**), (**??**), (**??**); partition sum (**??**); Ising (**??**); Gaussian (**??**).

5. Nonlinear lattice field theory

As we are writing this as a primer to our methods geared towards nonlinear lattice field theories, we choose to consider the most structurally simple of nonlinearities: Euclidean ϕ^k theory. First, we examine a continuum scalar, one-component field, d-dimensional Euclidean ϕ^k theory defined by action [121, 179, 216]

$$S[\Phi] = \int d^d x \left\{ \frac{1}{2}\left[\partial_\mu \phi(x)\right]^2 + \frac{\mu^2}{2}\,\phi^2(x) - \frac{g}{k!}\,\phi^k(x) \right\}\,, \tag{25}$$

with the Klein-Gordon mass $\mu \geq 0$, and the strength of the self-coupling $g \geq 0$. When working with nonlinear systems, we are really only interested in unstable orbits cite ChaosBook?. As this is the case, we have chosen our action to have the ϕ^k potential inverted when compared to more classical treatments. Doing this prevents the formation of stable orbits is this correct?.

When working on a discretized ϕ^k theory, the action is defined as the lattice sum over the Euclidean Lagrangian density and (25) becomes [163]

$$S[\Phi] = \sum_z \left\{ \frac{1}{2} \sum_{\mu=1}^{d} (\partial_\mu \phi)_z^2 + \frac{\mu^2}{2} \phi_z^2 - \frac{g}{k!} \phi_z^k \right\} , \tag{26}$$

where we have set lattice constant $a = 1$ throughout. In the spirit of anti-integrability [13], we split the action into 'kinetic' and local 'potential' parts $S[\Phi] = -\frac{1}{2}\Phi^\top \Box \Phi + V[\Phi]$, where the nonlinear self-interaction is contained in

$$V[\Phi] = \sum_z V(\phi_z) , \qquad V(\phi) = \frac{1}{2} \mu^2 \phi^2 - \frac{g}{k!} \phi^k , \quad k \geq 3 \tag{27}$$

with $V(\phi_z)$ a nonlinear potential, intrinsic to the lattice site z. The part bilinear in fields is the free field theory action

$$S_0[\Phi] = \frac{1}{2} \Phi^\top \left(-\Box + \mu^2 \mathbb{1} \right) \Phi , \tag{28}$$

Here the lattice Laplacian

$$\Box \phi_z = \sum_{||z'-z||=1} (\phi_{z'} - \phi_z) = -2d \, \phi_z + \sum_{||z'-z||=1} \phi_{z'} \quad \text{for all } z, z' \in \mathcal{L} \tag{29}$$

is the average of the lattice field variation $\phi_{z'} - \phi_z$ over the sites nearest to the site z. For a hypercubic lattice in one and two dimensions this discretized Laplacian is given by

$$\Box \phi_t \ = \phi_{t+1} - 2 \phi_t + \phi_{t-1} \tag{30}$$

$$\Box \phi_{jt} = \phi_{j,t+1} + \phi_{j+1,t} - 4 \phi_{jt} + \phi_{j,t-1} + \phi_{j-1,t} . \tag{31}$$

As we have now defined an action, we can write down the lattice Euler Lagrange equation which we can solve with periodic boundary conditions in order to determine the periodic orbits central to our theories of nonlinear dynamics.

First, we note that $\Box \equiv -\partial^T \partial$ because $\Box$ is the lattice Laplacian which, in finite difference notation, is given by $\Box = \frac{1}{a^2} \left(\sigma^{-1} - 2I - \sigma \right)$ and $\partial^T \partial = \frac{1}{a^2} \left(\sigma^{-1} - I \right) (\sigma - I) = \frac{1}{a^2} \left(2I - \sigma - \sigma^{-1} \right)$ this probably needs to be explained in an appendix a bit. Where σ is a matrix which rotates the lattice state forward by one lattice point. Now, if we take.

$$(\partial_\mu \phi)^T \partial_\mu \phi = \phi \partial_\mu^T \partial_\mu \phi = -\phi \Box \phi \tag{32}$$

Using (32) we can write our action (26) as

$$S[\phi] = \sum_\mu \frac{1}{2} (\partial_\mu \phi)^2 + V(\phi) = \sum_\mu -\frac{1}{2} \phi \Box \phi + V(\phi) \tag{33}$$

This should encompass all our Hamiltonian field theories (those that are non-dissipative can be treated through an action formulation). Now, the functional derivative commutes with the partial derivatives present in $\Box$, and $\Box$ is self-adjoint, so it works the same acting from the right as it does acting from the left. Therefore, we can write

$$\frac{\delta S[\phi]}{\delta \phi} = \sum_{\mu} -\frac{1}{2}\phi\Box - \frac{1}{2}\Box\phi + V'(\phi) = 0 \tag{34}$$

Summing over independent directions to get zero implies that each member of the sum is zero, so we get

$$-\Box\phi + V'(\phi) = 0 \tag{35}$$

as our lattice Euler–Lagrange equations.

[2023-06-26 Predrag] Use: symmetric difference equations of the form

$$\phi_{n+l} - f(\phi_n) + \phi_{n-1} = 0 \tag{36}$$

the Frenkel-Kontorova model which is equivalent to the area-preserving Chirikov-Taylor standard mapping.

[2023-07-07 Predrag] to Xanqui: please svn add your new section `symmetry.tex` to the repo.

For a two-dimensional square lattice, there are four classes of symmetry transformations: discrete translations $T = \{r_1^{m_1} r_2^{m_2}\}$, 90^o rotations around the origin $\{C, C^2, C^3\}$, even reflections (see the companion paper I [137] for details) across the spatial or temporal axis (time reversal, spatial reflection) $\{\sigma,\, \sigma_2\}$, and odd reflections across a diagonal (space-time interchange) $\{\sigma_1,\, \sigma_3\}$. The square lattice space group G thus consists of the translation subgroup (**??**), $T = \mathrm{C}_{\infty,1} \otimes \mathrm{C}_{\infty,2}$, and the 8-element dihedral point-group g,

$$\mathrm{D}_4 = \{e, C, C^2, C^3, \sigma, \sigma_1, \sigma_2, \sigma_3\}\,. \tag{37}$$

In the international crystallographic notation, this square lattice space group is referred to as *p4mm* [63].

We will be closely investigating two ϕ^k theories: the aforementioned ϕ^4, and ϕ^3. ϕ^4 has wide application in quantum field theory needs citations and thus understanding its behavior from a nonlinear dynamics perspective would be extremely useful. ϕ^3 on the other hand, is less useful for qft due to the non-normalizability of its potential, but its close connection to the well-studied temporal Hénon (Appendix A) allows us to explore many properties analytically, and even draw global conclusions about our field theory formulation in general. This paper will exclusively concern itself with one-dimensional theories, this follows along with our effort to build up understanding of chaotic spatiotemporal field theories in chunks cite LC21 and CL18. In the following sections we develop both ϕ^3 and ϕ^4 from (26), some general properties of each theory are developed followed by a discussion on "shadow states" and the symmetries of each system. With all this information, we are able to use Newton's method to extremely accurately and quickly determine cycles of up to length ?? for each theory.

6. Dynamics in state space

Before discussing global properties for non-linear systems, it is conventional to take a dynamical point of view and start with local forward-in-time formulation in state space. Later this notion of local will be connected with a global picture.

Field theory is closely related with the study of dynamical system. However, such connection is not always clearly illustrated. Thus, a rigorous and detailed discussion of underlying mathematics is favorable here.

6.1. Preliminary definitions

To conform with tradition in dynamical system, let $\mathcal{M}$ be state space that contains all possible field values, and $f : \mathcal{M} \times \mathcal{M} \to \mathcal{M}$ a self-homeomorphism on $\mathcal{M}$ is corresponding discrete time evolution operator that satisfies semi-group property of time evolution, which is defined inductively

$$
\begin{aligned}
f^n &= f \circ f^{n-1} \\
f^0 &= id_{\mathcal{M}} \,.
\end{aligned}
$$

In such a system $(\mathcal{M}, f)$, an invariant subset $A \subset \mathcal{M}$ is a set such that

$$
f(A) = A \tag{38}
$$

Examples of invariant subset are fixed points, limit cycles (as periodic orbits), ω-limits, etc. These invariant subsets has drawn great attention in the study of complicated dynamical systems. Among them, the most helpful ones are stable (unstable) manifolds, which are defined based on fixed points,

$$
\begin{aligned}
W^s(f,p) &= \{q \in \mathcal{M} | f^n(q) = p, n \to \infty\} \\
W^u(f,p) &= \{q \in \mathcal{M} | f^{-n}(q) = p, n \to \infty\} \,,
\end{aligned}
$$

where superscripts s and u indicates stable and unstable respectively. In other words, stable/unstable manifolds are points attracted or repelled by the fixed point p.

> [2024-02-08 Predrag] Changed the reference in "paper in 2017, Anastassiou *et al* rf Anastassiou17", please correct this if you mean another paper.

Anastassiou *et al* [7] used parameterization method to visualize stable/unstable manifolds for ϕ^4 theory and calculated homoclinic tangency. Locally near fixed points, the stable/unstable manifolds are locally straightened near fixed points with slopes determined by eigenvectors of Jacobian matrix (which is very reasonable as they agree in the tangent space at fixed points).

As introduced by Birkhoff[??] to strictly define dissipative systems, non-wandering set has been another important invariant subset in open systems where some solutions 'escape' from $\mathcal{M}$ and never return. The non-wandering set is defined as the complement of wandering set []. A point $x_0 \in \mathcal{M}$ is wandering if there exists a positive integer $N \in \mathbb{N}$ such that

[2024-02-08 Predrag] If father Birkhoff really introduced this, give a precise reference.

$$\exists U \ni x_0,\ f^n(U) \cap U = \emptyset\ \forall n > N \tag{39}$$

which means that after finitely many iterations, this neighborhood of x is never visited by this given solution anymore (similar to transitive solution in Markov process). Thus, the wandering set $\mathcal{W}$ is defined as

$$\mathcal{W} = \{x \in \mathcal{M} | x \text{ is wandering } \} \tag{40}$$

Correspondingly, the non-wandering set can be defined as $\mathcal{N} = \mathcal{M} \setminus \mathcal{W}$. In fact, non-wandering set of an open system is usually extremely complicated as zero-measure fractal with empty interior [53]. However, a finite-level rough visualization is available by the idea of Smale's horseshoe map. The usual practice is to take a large enough square cover near origin and map it forward and backward in time to intersect itself. Nevertheless, this practice seems rather artificial, since a square is in no way natural to the dynamics. A better approach is the find cover that is bounded by invariant manifolds instead (referred to as optimal cover later). This method is demonstrated using example of ϕ^3 and ϕ^4 in the following section.

In strong coupling regime, many physically important systems are characterized mathematically by Axiom A, which satisfies:

$$\begin{aligned} &(i)\ \ \Omega(f)\text{is compact} \\ &(ii)\ \text{The set of periodic point is dense in}\Omega(f) \end{aligned}$$

For any surface, hyperbolicity of non-wandering implies density, thus sometimes hyperbolic and axiom A are used interchangeably. The density of Axiom A diffeomorphism ensures that there exists an open neighborhood of $U \supset \Omega(f)$ and

$$\Omega(f) = \bigcap_{z \in \mathrm{Z}} f^z(U) \tag{41}$$

is a locally maximal invariant set for f. This is important for visualization technique of non-wandering set. An Axiom A diffeomorphism also supports a Markov partition [31] that lays basis for definition of symbolic dynamics.

As another important dynamical concept, hyperbolicity is characterized by local properties of tangent bundle. A differentiable map f is said to have hyperbolic structure on subset $\Lambda \subset \mathcal{M}$ if its tangent space can be decomposed into a direct sum of contracting and expanding directions at every point in Λ. Formally, Λ is a hyperbolic set if $\forall x \in \Lambda$,

$$\begin{aligned} &(i)\ \ \ T_x M = E^s_x \bigoplus E^u_x \\ &(ii)\ \ d_x f(E^{s,u}_x) = E^{s,u}_{f(x)} \\ &(iii)\ |d_x f|_{E^s_x} < \lambda_1,\ |d_x f^{-1}|_{E^u_x} < 1/\lambda_2,\ (0 < \lambda_1 < 1 < \lambda_2)\,, \end{aligned}$$

which means that $E^{s,u}_x$ are subspaces that are invariant under differential of f and represent contraction and expansion respectively.

6.2. Dynamical formulation on non-linear field theories

Such formal discussion of dynamical systems would be meaningless if we cannot associate the non-linear field theories of interest a dynamical formulation. Indeed, it is as natural as the transition from Lagrangian to Hamiltonian for any field theories at hand. Limiting ourselves on the highly nontrivial one-dimensional deterministic field theories, state space is $\mathcal{M} = \mathbb{R}^2$ due to three-term recurrence relation of ϕ^3 and ϕ^4(ref). Any point (represent a unique orbit) in $\mathcal{M}$ can be thought as given by it initial conditions (ϕ_0, ϕ_1) or (ϕ_0, φ_0) where $\varphi_t = \phi_{t+1}$. Time evolution is given by field equation $\phi_{t+1} = g(\phi_t, \phi_{t-1})$, written in vector form as

$$\hat{f}(\hat{\phi}_t) = \hat{f}\,(\,\varphi\,)_t \qquad \phi_t = (\,\phi\,)_t \qquad g(\phi_t, \varphi_t) = (\,\phi\,)_t \qquad \phi_{t+1} = \hat{\phi}_{t+1} \tag{42}$$

This operator $\hat{f}$ is completely specified by $g : \mathbb{R}^2 \to \mathbb{R}$, and for ϕ^3 and ϕ^4 it is given by

$$\begin{aligned} g(\phi_t, \phi_{t-1}) &= -\phi_{t-1} + \mu^2(-1/4 + \phi_t^2) + 2\phi_t \quad (\phi^3) \\ g(\phi_t, \phi_{t-1}) &= -\phi_{t-1} - \mu^2\phi_t^3 + (\mu^2 + 2)\phi_t \quad (\phi^4) \end{aligned} \tag{43}$$

This dynamical formulation gives a way to look at local properties like Jacobian matrix $\mathbb{J}$ or to inspect conditions for hyperbolicity in non-linear field theories. As temporal ϕ^3 theory is conjugate to the famous Henon map, studies on sufficient condition of hyperbolicity had been rich, and we just take result $a > 5.699310786700...$, which correspond to $\mu^2 > 5.17661....$ This makes us take $\mu^2 = 5.5$ for the rest discussion on ϕ^3 theory. In case of ϕ^4 theory, although it has attracted much attention in quantum field theory, the dynamical counterpart of ϕ^4 theory (which is a cubic map) is not as well investigated as Hénon, but a lot of efforts has been devoted to find a lower bound, similar to the bound of parameter a given. We adopt criterion from (ref) and take $\mu^2 = 3.5$ for our discussion on ϕ^4 theory, whose hyperbolicity can also be shown graphically in the next section through the existence of a transversal homoclinc point.

6.3. Homoclinic tangle

Another important insight from dynamical system is homoclinic tangle, first proposed by Poincare to account for the complicated behavior of evolution operator. More speficially, Smale-Birkhoff theorem suggests that the existence of a transversal homoclinic point implies the existence of an invariant Cantor set, and the dynamics on which is topologically conjugate to a m-symbol full shift. This notion of m-symbol full shift was later formalized by Smale as symbolic dynamics.

Compare to the mathematically rigorous discussion of existence of non-wandering set, this homoclinic tangle is much more intuitive, as it can be visualized through invariant manifolds , but we insisted that a detailed description of hyperbolicity and Axiom-A is necessary, as they can promote a natural way to visualize non-wandering set through intersections of a cover U of the non-wandering set. Here we propose a cover

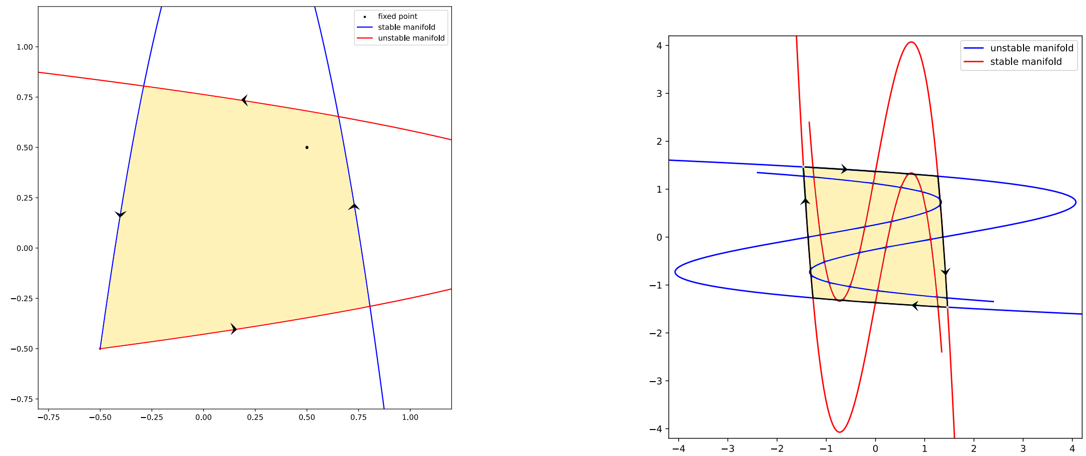

(a) Optimal cover of ϕ^3 theory with $\mu^2 = 5.5$

(b) Optimal cover of ϕ^4 theory with $\mu^2 = 3.5$

Figure 1: Visualization of optimal covers for ϕ^3 and ϕ^4 theory. Blue color indicates unstable manifold; red color indicates stable manifold; arrows indicates direction of expansion and contraction of invariant manifolds under time evolution f.

that is dynamically determined by the system, which we will call optimal cover in the following discussion.

6.4. Visualizing non-wandering set for ϕ^3 and ϕ^4

The key construction of an optimal cover of non-wandering set is to find a region that covers non-wandering set and whose boundary is invariant. This case is clearly illustrated by ϕ^3 example in Fig.1a, where the optimal cover is a region bounded by stable and unstable manifolds of fixed point origin. For ϕ^4, it is more complicated, as stable and unstable manifold from any of the fixed points cannot bound the non-wandering set. However, considering the internal symmetry ($\phi \to -\phi$) exhibited by ϕ^4 potential, invariant manifolds are not the only invariant subset that can serve as boundary. Period-2 orbits are pairwise degenerated after quotient of internal symmetry, and a union of their corresponding invariant manifolds (which can be thought as manifolds for evolution f^2) is also an invariant subset of M under f. Thus, for ϕ^4, optimal cover is bounded by the invariant manifolds associated with period 2 orbits, as illustrated in Fig.1b.

With the given optimal cover, approximation of non-wandering set follows 'bend and intersection' procedure of Smale's horseshoe map [], where diffeomorphism f is time evolution operator. Schematic plots Fig.2a Fig.**??** show how optimal covers are bent through a "stretch and fold" process.

The conjugation of time evolution in Ω and a m-symbol full-shift is manifested by a

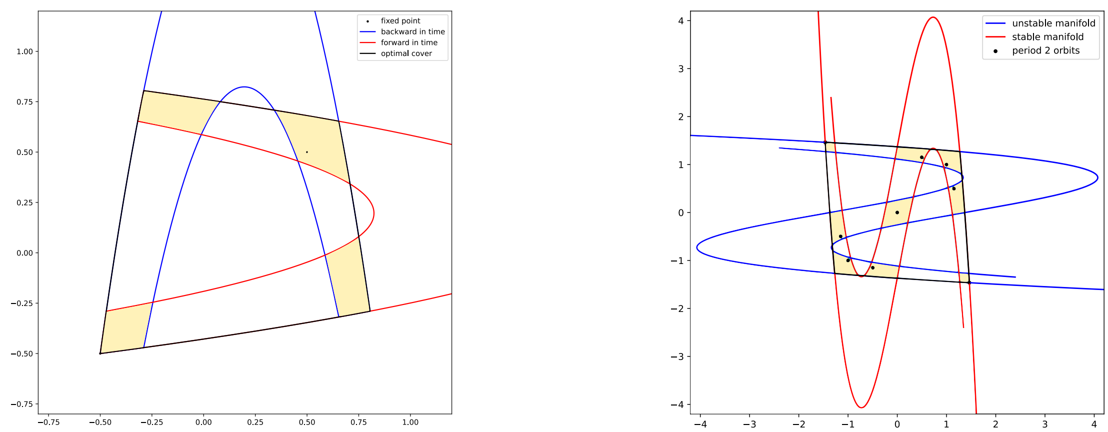

(a) "Stretch & fold" dynamics of ϕ^3 theory with $\mu^2 = 5.5$

(b) "Stretch & fold" dynamics of ϕ^4 theory with $\mu^2 = 3.5$

Figure 2: Schematics plots of how Ω is constructed through a dynamical process topologically equivalent to Smale's horseshoe

closer look at $f(N)\cap N$ and $f^{-1}(N)\cap N$ in Fig.2. In general, time evolution of ϕ^k theory conjugates to k-1 symbols, as $f(N)$ is divided by N into k-1 simply connected regions in $\mathbb{R}^2$ where k-1 symbols can be assigned, the construction of which is reminiscent of Cantor set. Following the time evolution, $f^2(N)\cap N$ consists of $(k-1)^2$ simply-connected regions, with each region represented by a length-2 string with k-1 symbols, and $f^n(N)\cap N$ $(k-1)^n$ regions represented by length-n strings. Thus, we construct a sequence of nested sets (as finite approximations of Ω) $\{\Omega_n\}$ such that

$$\Omega_n = (f^n(N)\cap N)\cap(f^{-n}(N)\cap N), \quad (\Omega_n \subset \Omega_{n'} \forall n > n') \tag{44}$$

The structure of invariant set (which is the limit of this nested sequence) $\Omega = \lim_{n\to\infty}\bigcap \Omega_n$ is revealed by the sequence of $\{\Omega_n\}$. Write $\Omega_n = (f^n(N)\cap N)\cap(f^{-n}(N)\cap N)$, it is clear that $f^n(N)\cap N$ resembles the construction of Smale's horseshoe map, where the existence of a transversally homoclinic point guarantees that $f^n(N)\cap N$ is a disjoint union of $(k-1)^n$ simply connected regions (for ϕ^k theory, with our example taking $k=3,4$), each being compact. Therefore, we can label the $(k-1)^{2n}$ disjoint connected regions in Ω_n (as an intersection of $f^n(N)\cap N$ and its reversed image) by a length 2n string with $k-1$ symbols.

$$\Omega_n = \bigsqcup_{s\in S_n} \Omega_n^s\,,\ S_n = \mathcal{A}^{2n}\,,\ |\mathcal{A}| = k-1 \tag{45}$$

We arrange the symbol strings in such a way that if $s = s_{-n+1}s_{-n+2}...s_0s_1...s_n$ and $s' = s'_{-m+1}s'_{-m+2}...s'_0s'_1...s'_m$ $(n > m)$ and $s_k = s'_k$ $(\forall|k| \leq m)$, then $\Omega_n^s \subset \Omega_m^{s'}$ (which is possible because $\{\Omega_n\}$ is a nested sequence). Notice that we construct a Markov partition $\{\Omega_n^s\}_{s\in S_n}$ at each finite approximation Ω_n, which is the famous result prove by Bowen in 1975. With this arrangement, for each bi-infinite string $s = ...s_{-1}s_0s_1s_2... \in S = \mathcal{A}^{\mathbb{Z}}$, we can construct a sequence of nested compact sets $\{\Omega_n^{s^n}\}$ where $s^n = s_{-n+1}...s_0s_1...s_n$ denote the finitely truncated substring of s of length 2n. Let $\Omega^s = \lim_{n\to\infty}\bigcap\Omega_n^{s^n}$, by Cantor's intersection theorem Ω^s is non-empty. Since Ω is the disjoint union of Ω^s

$$\Omega = \bigsqcup_{s\in\mathcal{A}^{\mathbb{Z}}} \Omega^s \tag{46}$$

and Ω is, by its fractal nature, a totally disconnected, whose connected components are only singletons, we conclude that every orbit in Ω is uniquely represented by a bi-infinite string in S. By far, we have constructed a bijection between Ω and S, and it is clear that the time evolution (restricted on Ω) $f|_\Omega : \Omega \to \Omega$ is represented by a shift in S (and bijection guarantees it to be a full shift).

In this process as lies the important fact $\bar{P} = \Omega$, where P is the set of all periodic solutions and the bar means closure (mathematically speaking the smallest close set that contains P). Since the "diameter" of Ω^s decreases as the length of s increases, we can conclude that in an arbitrarily small neighborhood of $x \in \Omega\backslash P$ there is a periodic solution $c \in P$. The correspondence between $\bar{P}$ and Ω (both as finite approximations) is shown in Fig.3 for both ϕ^3 (left panel) and ϕ^4 (right panel). This figure shows all periodic states up to period 7 and $f^2(N)\cap f^{-2}(N)$. There is a clear self-similar structure for these periodic orbits, and expected correspondence between these two sets is clear.

In a metric space (like $\mathbb{R}^2$), all the points $x \in \bar{P}\backslash P$ are said to have 'zero distance' with P, which means that for any $\delta > 0$, we can find $c \in P$ such that $d(x, c) < \delta$. We will say that c shadows x with precision δ. The existence of shadowing is the solid foundation of cycle expansion for dynamics zeta function, which will be thoroughly explored in the next section.

Through the visualization process, it is becomes clear that for a certain range of parameter (when homoclinic tangency exists), ϕ^k theory is an Axiom A flow and possess hyperbolicity on the locally maximal invariant set Ω. The dynamics on Ω is thus conjugated to a $k-1$ symbol full shift, and this enables us to use shadowing (i.e. exploit the properties of Ω by calculation based on P) in cycle expansion of dynamical zeta function.

[2023-06-26 Predrag] What follows is `spatiotemp/chapter/phi4latt.tex`. Temporary, until phi4.tex is finalized.

7. Deterministic ϕ^3 lattice field theory

Consider the non-Laplacian part of the action (26), with cubic Biham-Wenzel [27] lattice site potential (27)

$$V(\phi) = \frac{\mu^2}{2}\,\phi^2 - \frac{g}{3!}\,\phi^3 = -\frac{g}{3!}\Big(\phi^3 - 3\lambda\,\phi^2\Big)\,, \quad \lambda = \mu^2/g\,, \tag{47}$$

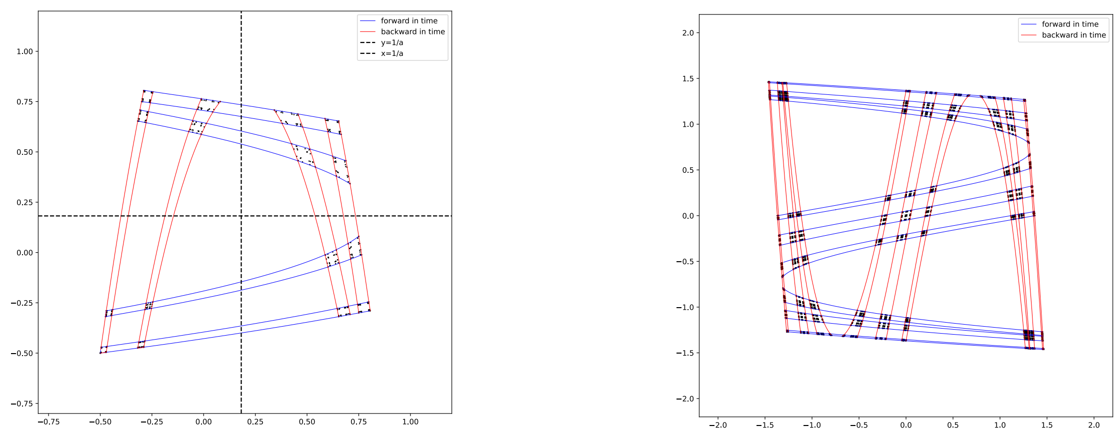

(a) Approximation of Ω_2 and P for ϕ^3 theory with $\mu^2 = 5.5$

(b) "Approximation of Ω_2 and P for ϕ^4 theory with $\mu^2 = 3.5$

Figure 3: Schematics plots of the correspondence between Ω and $\bar{P}$, where the self-similar structure of Cantor set is cleared presented

parametrized by the Klein-Gordon mass $\mu > 0$ and the self-coupling constant $g \geq 0$. We will scale away one of the two parameters, in two ways. In section 7.1 we shall bring the theory to the normal, Hénon form. Here we bring it to the anti-integrable [12, 13, 196] form, suitable for the analysis of theory's strong coupling limit.

We start by a field translation $\phi \to \phi + \epsilon$:

$$-\frac{g}{3!}\Big((\phi+\epsilon)^3 - 3\lambda(\phi+\epsilon)^2\Big) = -\frac{g}{3!}\Big(\phi^3 + 3(\epsilon-\lambda)\phi^2 + 3\epsilon(\epsilon-2\lambda)\phi\Big) + (\text{const})\,.$$

Choose the field translation $\epsilon = \lambda$, such that the ϕ^2 term vanishes,

$$-\frac{g}{3!}(\phi^3 - 3\lambda^2\phi) + (\text{const})\,.$$

Drop the (const) term, and rescale the field $\phi \to 2\,\lambda\,\phi$:

$$-4\lambda^2\mu^2\Big(\frac{\phi^3}{3} - \frac{\phi}{4}\Big)\,.$$

The ϕ^3 scalar field theory action (26) takes form

$$S[\Phi] = \sum_z \left\{-\frac{1}{2}\phi_z\Box\phi_z - \mu^2\Big(\frac{\phi_z^3}{3} - \frac{\phi_z}{4}\Big)\right\}\,. \tag{48}$$

The Euler–Lagrange equation (8) for the scalar lattice ϕ^3 field theory is now, in the $d=1$ temporal lattice case

$$-\phi_{t+1} + 2\,\phi_t - \phi_{t-1} \;+\; \mu^2(-\phi_t^2 + 1/4) \;=\; 0\,, \tag{49}$$

and in the d-dimensional spatiotemporal lattice case,

[2024-03-07 Predrag] Removed prefactor $1/d$ from the Laplacian here.

$$\sum_{||z'-z||=1} (\phi_{z'} - \phi_z) \;-\; \mu^2 \, (\phi_z^2 - 1/4) \;=\; 0 \,, \tag{50}$$

parametrized by a *single* parameter, the Klein-Gordon mass μ^2, with the "coupling constant" g in (26) scaled away.

Next, we compute the period-1 and period-2 periodic states.

Period-1 periodic states. From the Euler–Lagrange equation (49) it follows that the period-1, constant periodic states, $\phi_t = \overline{\phi}$, for the $d = 1$ lattice are the zeros of function

$$F[\overline{\phi}] = \frac{4\mu^6}{g^2}\Big(\overline{\phi}^2 - \frac{1}{4}\Big) \,, \tag{51}$$

with two real roots $\overline{\phi}_m$

$$(\overline{\phi}_L, \overline{\phi}_R) = \Big(-\frac{1}{2}, \frac{1}{2}\Big) \,. \tag{52}$$

Period-2 periodic states. To determine the four period-2 periodic states $\overline{\Phi}_m = \overline{\phi_0\phi_1}$, set $x = \phi_{2k}$, $y = \phi_{2k+1}$ in the Euler–Lagrange equation (49), and seek the zeros of

$$F[x, y] = \begin{pmatrix} 2(x-y) - \mu^2(x^2 - 1/4) \\ 2(y-x) - \mu^2(y^2 - 1/4) \end{pmatrix} . \tag{53}$$

That is best done using the Friedland and Milnor [84] 'the center of gravity' and Endler and Gallas [71, 72] 'center of mass' or 'orbit' polynomials, but for the period-2 periodic states it suffices to eliminate y using $F_1 = 0 \Rightarrow y(x) = x - \frac{\mu^2}{2}(x^2 - 1/4)$, and seek zeros of the second component,

$$F_2[x, y(x)] = -\mu^2\Big(x - \frac{1}{2}\Big)\Big(x + \frac{1}{2}\Big)\Big(\frac{\mu^4}{4}x^2 - \mu^2 x + \Big(2 - \frac{\mu^4}{16}\Big)\Big) \tag{54}$$

The first 2 roots are the $x = y$ period-1 periodic states (52). There is one period-2 periodic state $\overline{12}$

$$x, y = \frac{2 \pm 2\sqrt{\frac{\mu^4}{16} - 1}}{\mu^2} \,, \tag{55}$$

so the prime period-2 periodic state exists for $\mu^2 > 4$. For $\mu^2 = 4$ the period-2 periodic states pairs coalesce with the positive period-1 periodic states

$$F_2[x, y(x)] = -4(x^2 - \frac{1}{4})(x^2 - \frac{1}{2})^2 \,. \tag{56}$$

In the anti-integrable limit [12, 13] $\mu \to \infty$, the site field values

$$F_2[x, y(x)] \to -\frac{\mu^6}{4}(x - \frac{1}{2})^2(x + \frac{1}{2})^2 \tag{57}$$

tend to the two steady states (52).

the orbit Jacobian matrix

$$\mathcal{J}_{zz'} = \; - \Box_{zz'} \; - \; 2\,\mu^2 \phi_z \, \delta_{zz'} \,, \tag{58}$$

7.1. Spatiotemporal lattice Hénon theory

The primary advantage of studying ϕ^3 is that it can readily be connected to the well studied temporal Hénon map needs citations. We can see this connection through a straightforward linear transformation. As temporal Hénon is most commonly studied in one-dimension, for the following analysis d in (50) will be set to 1. To transform between ϕ^3 and temporal Hénon we can apply the transformation $\phi_t = c\varphi_t + \varepsilon$ to (50), setting $\varepsilon = \frac{1}{\mu^2}$ yields

$$-\varphi_{t+1} - \mu^2 c\varphi_t^2 - \varphi_{t-1} = \frac{4-\mu^4}{4\mu^2 c} = 1$$

Where the last equality is a condition enforced to maintain the form of temporal Hénon with inverted lattice values ($\varphi \to -\varphi$). Finally, we set $-\mu^2 c = a$ to recover the classical temporal Hénon parameter. Solving our two conditions and enforcing that all binary symbolic dynamics are admissible with $a = 6$, we find $c = -\frac{2}{\sqrt{3}}$ and $\mu^2 = 3\sqrt{3}$. So, the transformation which brings ϕ^3 into temporal Hénon is

$$\phi = -\frac{2}{\sqrt{3}}\varphi + \frac{1}{3\sqrt{3}} \tag{59}$$

7.2. Biham-Wenzel potential

Biham and Wenzel [27] (see ChaosBook sect. 34.1 *Fictitious time relaxation*) construct a time-asymmetric cubic action

$$S[\Phi] = \sum_{t\in\mathbb{Z}} \left(\phi_{t+1}\phi_t - b\,\phi_t\phi_{t-1} + \frac{a}{3}\phi_t^3 - \phi_t\right)\,, \tag{60}$$

whose Euler–Lagrange equation is the temporal Hénon 3-term recurrence equation (**??**), with dissipation,

$$F_t[\Phi] = -\phi_{t+1} + b\,\phi_{t-1} - a\phi_t^2 + 1\,, \tag{61}$$

and the orbit Jacobian operator

$$\mathcal{J}_{zz'} = -r + b\,r^{-1} - 2a\phi_t\,. \tag{62}$$

With the cubic potential at lattice site n we can start to look for orbits variationally. Note that the potential is time-reversal invariant for $b = 1$.

> [2024-02-15 Sidney] For time being, I commented out states.tex here, have it in blogSVW.tex, until finalized. Will restore it. 2024-03-07 Predrag: Xuanqi just edited it, so I restored it.

8. Deterministic ϕ^4 lattice field theory

Consider the discrete scalar one-component field, d-dimensional ϕ^4 theory [185] defined by the Euclidean action (26)

$$S[\Phi] = \sum_z \left\{\frac{1}{2}\sum_{\mu=1}^{d}(\Delta_\mu\phi_z)^2 + \frac{\mu^2}{2}\,\phi_z^2 - \frac{g}{4!}\,\phi_z^4\right\}\,, \tag{63}$$

with the Klein-Gordon mass $\mu \geq 0$, quartic lattice site potential (27),

$$V(\phi) = \frac{1}{2}\,\mu^2\,\phi^2 - \frac{g}{4!}\,\phi^4\,, \tag{64}$$

the strength of the self-coupling $g \geq 0$, and we set lattice constant $a = 1$ throughout.

A popular way [145] to rewrite the quartic action (63) is to complete the square

$$V(\phi) = -\frac{g}{4!}\left(\phi_z^2 - 3!\,\frac{\mu^2}{g}\right)^2 + (\mathrm{const})\,,$$

drop the (const) term, and rescale the field $\phi_z^2 \to 3!\,\frac{\mu^2}{g}\phi_z^2$:

$$S[\Phi] = 3!\,\frac{\mu^2}{g}\sum_z \left\{ -\frac{1}{2}\phi_z\Box\phi_z - \frac{1}{4}\,\mu^2\left(\phi_z^2-1\right)^2 \right\}. \tag{65}$$

The Euler–Lagrange equation (27) for the $d = 1$ scalar lattice ϕ^4 field theory,

$$-\phi_{t+1} + [-\mu^2\,\phi_t^3 + (\mu^2+2)\,\phi_t] - \phi_{t-1} \;=\; 0\,, \tag{66}$$

is thus parametrized by a *single* parameter, the Klein-Gordon mass $\mu^2 = s-2$, with the “coupling constant” g in (63) scaled away. Next, we compute the period-1 and period-2 periodic states.

Period-1 periodic states. From the Euler–Lagrange equation (66) it follows that the period-1 periodic states, $\phi_t = \overline{\phi}$, for the $d = 1$ lattice are the zeros of function

$$F[\overline{\phi}] = \mu^2\,(1+\overline{\phi})\,\overline{\phi}\,(1-\overline{\phi})\,. \tag{67}$$

As long as the Klein-Gordon mass is positive, there are 3 real roots $\overline{\phi}_m$

$$(\overline{\phi}_L, \overline{\phi}_C, \overline{\phi}_R) = (-1, 0, 1)\,. \tag{68}$$

The period-1 primitive cell orbit Jacobian matrix $\mathcal{J}$ is a $[1\times 1]$ matrix

$$\mathcal{J} = d_m = \frac{dF[\phi]}{d\phi} = \mu^2\,(1-3\overline{\phi}_m^2) \;=\; \mu^2 \;\text{ or }\; -2\mu^2\,, \tag{69}$$

so the ”stretching” factor for the 3 steady periodic states is

$$(d_L, d_C, d_R) = (-2\mu^2, \mu^2, -2\mu^2)\,. \tag{70}$$

Period-2 periodic states. To determine the nine period-2 periodic states $\overline{\Phi}_m = \overline{\phi_0\phi_1}$, set $x = \phi_{2k}$, $y = \phi_{2k+1}$ in the Euler–Lagrange equation (66), and seek the zeros of

$$F[x,y] = \begin{pmatrix} -(s-2)x^3 + sx - 2y \\ -(s-2)y^3 + sy - 2x \end{pmatrix}. \tag{71}$$

That is best done using the Friedland and Milnor [84] ‘the center of gravity’ and Endler and Gallas [71, 72] ‘center of mass’ or ‘orbit’ polynomials, but for the period-2 periodic states it suffices to eliminate y using $F_1 = 0 \Rightarrow 2\,y(x) = -x^3 + sx$, and seek zeros of the second component,

$$F_2[x,y(x)] = \frac{\mu^8}{8}(x-1)\,x\,(x+1)\left(x^2-1-\frac{4}{\mu^2}\right)\left(x^4-(1+\frac{2}{\mu^2})x^2+\frac{4}{\mu^4}\right) \tag{72}$$

The first 3 roots are the $x = y$ period-1 periodic states (68). There is one symmetric period-2 periodic state $\overline{LR}$

$$x = -y = \pm\sqrt{1 + 4/\mu^2}\,, \tag{73}$$

and a pair of period-2 asymmetric periodic states $\overline{LC}$, $\overline{CR}$ related by reflection symmetry (time reversal).

For $\mu^2 = 2$ the period-2 asymmetric periodic states pairs coalesce with the two period-1 asymmetric periodic states

$$2\,x(x^2 - 3)(x^2 - 1)^3\,. \tag{74}$$

To get a complete horseshoe (all 3^n 3-symbol bimodal map itineraries are realized), you know what to do next (see figure 2. in [84]). Numerical work indicates [215] that for $\mu^2 > 2.95$ the horseshoe is complete.

In the anti-integrable limit [12, 13] $\mu \to \infty$, the site field values

$$F_2[x, y(x)] \to \frac{\mu^8}{8}(x+1)^3\,x^3\,(x-1)^3 \tag{75}$$

tend to the three steady states (68).

9. Shadow state, temporal Hénon

[2022-02-24 Predrag] The initial version, parametrized by Hénon map parameter a. Superseded by section 10. To be made into an appendix.

Have: a partition of state space $\mathcal{M} = \mathcal{M}_A \cup \mathcal{M}_B \cup \cdots \cup \mathcal{M}_Z$, with regions $\mathcal{M}_m$ labelled by an $|\mathcal{A}|$-letter finite alphabet $\mathcal{A} = \{m\}$. The simplest example is temporal Hénon partition into two regions, labelled '0' and '1',

$$m_t \in \mathcal{A} = \{0, 1\}\,, \tag{76}$$

plotted in figure 4 (b). Prescribe a symbol block M over a finite primitive cell of a d-dimensional lattice. A 1-dimensional example:

$$\mathsf{M} = (m_0, \cdots, m_{n-1})\,. \tag{77}$$

Want: the periodic state Φ_M whose lattice site fields ϕ_t lie in state space domains $\phi_t \in \mathcal{M}_m$, as prescribed by the given symbol block M. A 1-dimensional example:

$$\Phi_\mathsf{M} = (\phi_0, \cdots, \phi_{n-1})\,, \quad \phi_t \in \mathcal{M}_m\,, \tag{78}$$

By *periodic state* Φ we mean a point in the n-dimensional state space that is a solution of the defining Euler–Lagrange equation. For the temporal Hénon example, that equation is the 3-term recurrence (**??**),

$$-\phi_{t+1} + a\,\phi_t^2 - \phi_{t-1} = j_t\,, \quad j_t = 1\,, \tag{79}$$

with all $a = 6$ period-5 periodic states plotted in figure A1.

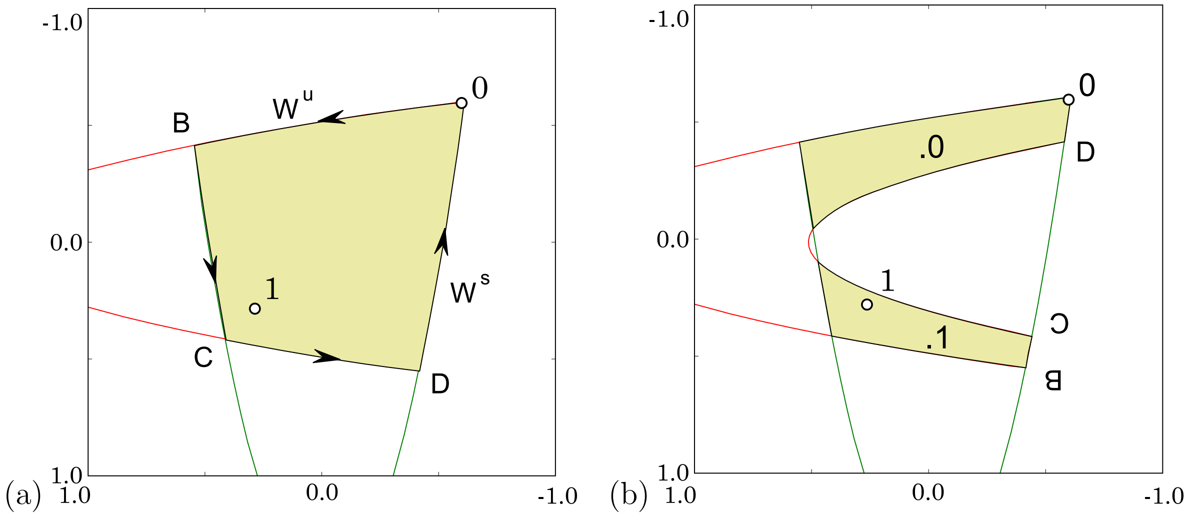

Figure 4: Temporal Hénon (A.1), (**??**) stable-unstable manifolds Smale horseshoe partition in the (ϕ_t, ϕ_{t+1}) plane for $a = 6$, $b = -1$: fixed point $\overline{0}$ with segments of its stable, unstable manifolds W^s, W^u, and fixed point $\overline{1}$. The most positive field value is the fixed point ϕ_0. The other fixed point ϕ_1 has negative stability multipliers, and is thus buried inside the horseshoe. (a) Their intersection bounds the region $\mathcal{M}_. = 0BCD$ which contains the non–wandering set Ω. (b) The intersection of the forward image $f(\mathcal{M}_.)$ with $\mathcal{M}_.$ consists of two (future) strips $\mathcal{M}_{0.}$, $\mathcal{M}_{1.}$, with points BCD brought closer to fixed point $\overline{0}$ by the stable manifold contraction. (The same as ChaosBook fig. 15.5, with $\phi_t = -x_t$.)

Shadow state method. Periodic states are the skeleton for dynamics in the uniformly invariant subset, thus it is necessary that we have a systematic algorithm to find periodic states numerically. One of the most powerful method among such is shadow state method, which involves constructing a shadow state based on symbolic dynamics as the initial guess and the minimize the deviation function.

Construct a *shadow state* $\overline{\Phi}_{\mathsf{M}}$ and the *forcing* $j(\mathsf{M})_t$ such that the site-by-site deviation

$$\varphi_t = \phi_t - \overline{\phi}_t \tag{80}$$

is small. Determine the desired periodic state Φ_{M} as the neighboring $|\Phi_{\mathsf{M}} - \overline{\Phi}_{\mathsf{M}}|$ fixed point of the M-forced Euler–Lagrange equation.

Desideratum: Plot the first, $n = 6$ temporal Hénon asymmetric periodic state Φ_{M} and shadow state $\overline{\Phi}_{\mathsf{M}}$, to illustrated the idea.

First, determine the fixed points (solutions with a constant field on all lattice sites) $\phi_t = \overline{\phi}_m$. For temporal Hénon there are two, $\overline{\phi}_0$ and $\overline{\phi}_1$ (see figure 4), labeled by the alphabet (76).

Next, construct the simplest configuration from $|\mathcal{A}|$ fields $\overline{\phi}_m$, each field in the domain of state space prescribed by the symbol block M. In the shadow state method,

$m_{t-1}m_tm_{t+1}$	$\bar{j}(\mathsf{M})_t$		
0 0 0	0		
0 0 1 = 1 0 0	-A	=	$\bar{\phi}_1 - \bar{\phi}_0$
0 1 0	-B	=	$a(\bar{\phi}_1^2 - \bar{\phi}_0^2)$
1 0 1	B	=	$a(\bar{\phi}_0^2 - \bar{\phi}_1^2)$
1 1 0 = 0 1 1	A	=	$\bar{\phi}_0 - \bar{\phi}_1$
1 1 1	0		

Table 1: Temporal Hénon fixed-points shadow state $\bar{\Phi}_{\mathsf{M}}$ forcing $\bar{j}(\mathsf{M})_t$ depends on the t lattice site and its two neighbors $m_{t-1}m_tm_{t+1}$. It takes values $(0, \pm A, \pm B)$. If period-2 or longer periodic states are utilized as shadows, more neighbors contribute.

we pick a fixed point $\bar{\phi}_m$ in each domain as domain's representative $\bar{\phi}_m \in \mathcal{M}_m$. For the temporal Hénon example, the fixed-points *shadow state* is:

$$\bar{\Phi}_{\mathsf{M}} = (\bar{\phi}_0, \cdots, \bar{\phi}_{n-1})\,, \qquad \text{where } \bar{\phi}_t = \begin{cases} \bar{\phi}_0 \text{ if } m_t = 0 \\ \bar{\phi}_1 \text{ if } m_t = 1 \end{cases} . \tag{81}$$

In general, the shadow state $\bar{\Phi}_{\mathsf{M}}$ does not satisfy the Euler–Lagrange equation (79), violating it by amount $\bar{j}(\mathsf{M})_t$

$$-\bar{\phi}_{t+1} + a\,\bar{\phi}_t^2 - \bar{\phi}_{t-1} = 1 - \bar{j}(\mathsf{M})_t\,, \tag{82}$$

where the forcing $\bar{j}(\mathsf{M})_t$ depends on $\bar{\phi}_t$ and its neighbors. For the temporal Hénon example, it takes the values tabulated in table 2.

Subtract (91) from (79) to obtain the 3-term recurrence for $\varphi_t = \phi_t - \bar{\phi}_t$, the deviations (89) from the shadow state,

$$-\varphi_{t+1} + a\,(\phi_t^2 - \bar{\phi}_t^2) - \varphi_{t-1} = \bar{j}(\mathsf{M})_t\,.$$

Substituting $\phi_t^2 = (\varphi_t + \bar{\phi}_t)^2$ and $j(\mathsf{M})_t = \bar{j}(\mathsf{M})_t - a\,\bar{\phi}_t^2$, we obtain

M*-forced Euler–Lagrange equation*

for the deviation φ_{M} from the shadow lattice state configuration $\bar{\Phi}_{\mathsf{M}}$:

$$-\varphi_{t+1} + a\,(\varphi_t + \bar{\phi}_t)^2 - \varphi_{t-1} = j(\mathsf{M})_t\,. \tag{83}$$

[2022-02-22 Predrag] Clearly I have to recompute the violation table table 2, but that's for another day.

This is to be solved by whatever code you find optimal. For example:

Vattay inverse iteration (C.1) is now

$$\varphi_t^{(m+1)} = -\bar{\phi}_t + \sigma_t \frac{1}{\sqrt{a}} \left(j(\mathsf{M})_t + \varphi_{t+1}^{(m)} + \varphi_{t-1}^{(m)} \right)^{1/2} , \tag{84}$$

and that should converge like a ton of rocks.

Perhaps watch *Shadow state conspiracy* (35:26 min)

Overview

(i) The M-forced Euler–Lagrange equation is *exact*, the only difference from the starting Euler–Lagrange equation (79) is that lattice fields ϕ_t have been translated by constant amounts (89) in order to center it on the M-th saddlepoint 'landscape'. There is one such M-forced Euler–Lagrange equation for each admissible symbol block M.

(ii) M-forced 3-term recurrence (92) is *exact*. It is superior to the original recurrence as it has built-in symbolic dynamics. The deviations $\varphi_t = \phi_t - \overline{\phi}_t$ should be small, and the topological guess based on M-forcing should be robust. The recurrence can be solved by any method you like.

(iii) ϕ^4 field theory works the same, with the M-forced 3-term recurrence for the deviations φ_t now built from approximate 3-field values $(\overline{\phi}_L, \overline{\phi}_C = 0, \overline{\phi}_R)$. If using Vattay (93), the Hénon sign σ_t needs to be rethought.

(iv) Implement M-forced 3-term recurrence for symmetric states boundary conditions.

(v) Generalization to higher spatiotemporal dimensions is immediate (see, for example, the 2-dimensional Vattay iteration (C.3)).

(vi) As one determines larger and larger primitive cell periodic states, on can use the already computed ones instead of the initial $(\overline{\phi}_0, \overline{\phi}_1)$ to get increasingly better M-forced shadowing.

(vii) The boring forcing term $j_t = 1$ on RHS of the temporal Hénon recurrence (79) has been replaced by a non-trivial forcing $j(\mathsf{M})_t$ in (92), as hoped for.

(viii) This is not the Biham-Wentzel method: it's based on exact Euler–Lagrange equations, there are no artificially inverted potentials, as we are not constructing an attractor; all our solutins are and should be unstable.

(ix) The Newton method requires evaluation of the orbit Jacobian matrix $\mathcal{J}$. As we have only *translated* field values $\phi_t \to \varphi_t$, $\mathcal{J}$ is the same as for the original 3-term recurrence. For large periodic states variational methods discussed below should be far superior to simple Newton.

(x) Have a look at Fourier transform of (92). Anything gained in Fourier space? Remember, we have not quotiented translation symmetry, we are still computing n periodic states on the spatiotemporal lattice.

(xi) Shadowing method was first formulated by Kai Hansen [95] in *Alternative method to find orbits in chaotic systems* (1995).

10. Shadow state, ϕ^3

[2022-02-24 Predrag] The rewrite of section 9, now parametrized by ϕ^3 parameter μ^2.

[2024-02-15 Sidney] Sidney rewrite for the current definition of ϕ^3, to replace siminos/tigers/state.tex when finalized here.

Have: a partition of state space $\mathcal{M} = \mathcal{M}_A \cup \mathcal{M}_B \cup \cdots \cup \mathcal{M}_Z$, with regions $\mathcal{M}_m$ labelled by an $|\mathcal{A}|$-letter finite alphabet $\mathcal{A} = \{m\}$. The simplest example is temporal ϕ^3 theory (which can be easily mapped into temporal Hénon via put equation here) which partitions its domain into two regions, labelled '0' and '1',

$$m_t \in \mathcal{A} = \{0, 1\} , \tag{85}$$

plotted in figure 4 (b). We can prescribe a symbol block M over a finite primitive cell of a d-dimensional lattice. A 1-dimensional example is:

$$\mathsf{M} = (m_0, \cdots, m_{n-1}) . \tag{86}$$

Want: the periodic state Φ_{M} whose lattice site fields ϕ_t lie in state space domains $\phi_t \in \mathcal{M}_m$, as prescribed by the given symbol block M. The one-dimensional temporal lattice case:

$$\Phi_{\mathsf{M}} = (\phi_0, \cdots, \phi_{n-1}) , \quad \phi_t \in \mathcal{M}_m , \tag{87}$$

By *periodic state* Φ we mean a point in the n-dimensional state space that is a solution of the defining Euler–Lagrange equation. For the ϕ^3 example example, that equation is the 3-term recurrence (**??**),

$$-\phi_{t+1} + 2\phi_t - \phi_{t-1} + \mu^2 \left(-\phi_t^2 + \frac{1}{4}\right) = j_t , \quad j_t = 0 , \tag{88}$$

with all $a = 6$ period-5 periodic states plotted in figure A1 (needs to be changed to ϕ^3).

Shadow state method. Construct a *shadow state* $\overline{\Phi}_{\mathsf{M}}$ and the *forcing* $j(\mathsf{M})_t$ such that the site-by-site deviation

$$\varphi_t = \phi_t - \overline{\phi}_t \tag{89}$$

is small. Determine the desired periodic state Φ_{M} as the neighboring $|\Phi_{\mathsf{M}} - \overline{\Phi}_{\mathsf{M}}|$ fixed point of the M-forced Euler–Lagrange equation.
Desideratum: Plot the first, $n = 6$ temporal Hénon asymmetric periodic state Φ_{M} and shadow state $\overline{\Phi}_{\mathsf{M}}$, to illustrated the idea.

First, determine the fixed points (solutions with a constant field on all lattice sites) $\phi_t = \overline{\phi}_m$. For temporal ϕ^3 there are two, $\overline{\phi}_0$ and $\overline{\phi}_1$ (see figure 4), labeled by the alphabet (76).

Next, construct the simplest configuration from $|\mathcal{A}|$ fields $\overline{\phi}_m$, each field in the domain of state space prescribed by the symbol block M. In the shadow state method, we pick a fixed point $\overline{\phi}_m$ in each domain as domain's representative $\overline{\phi}_m \in \mathcal{M}_m$. For the temporal ϕ^3 example, the fixed-points *shadow state* is:

$$\overline{\Phi}_{\mathsf{M}} = (\overline{\phi}_0, \cdots, \overline{\phi}_{n-1}) , \qquad \text{where } \overline{\phi}_t = \begin{cases} \overline{\phi}_0 \text{ if } m_t = 0 \\ \overline{\phi}_1 \text{ if } m_t = 1 \end{cases} . \tag{90}$$

$m_{t-1}m_tm_{t+1}$	$\overline{j}(\mathsf{M})_t$		
0 0 0	0		
0 0 1 = 1 0 0	-A	=	$\overline{\phi}_1 - \overline{\phi}_0$
0 1 0	-B	=	$2(\overline{\phi}_0 - \overline{\phi}_1) + \mu^2(\overline{\phi}_1^2 - \overline{\phi}_0^2)$
1 0 1	B	=	$2(\overline{\phi}_1 - \overline{\phi}_0) + \mu^2(\overline{\phi}_0^2 - \overline{\phi}_1^2)$
1 1 0 = 0 1 1	A	=	$\overline{\phi}_0 - \overline{\phi}_1$
1 1 1	0		

Table 2: Temporal ϕ^3 fixed-points shadow state $\overline{\Phi}_{\mathsf{M}}$ forcing $\overline{j}(\mathsf{M})_t$ depends on the t lattice site and its two neighbors $m_{t-1}m_tm_{t+1}$. It takes values $(0, \pm A, \pm B)$. If period-2 or longer periodic states are utilized as shadows, more neighbors contribute.

In general, the shadow state $\overline{\Phi}_{\mathsf{M}}$ does not satisfy the Euler–Lagrange equation (79), violating it by amount $\overline{j}(\mathsf{M})_t$

$$-\phi_{t+1} + 2\phi_t - \phi_{t-1} + \mu^2\left(-\phi_t^2 + \frac{1}{4}\right) = -\overline{j}(\mathsf{M})_t\,, \tag{91}$$

where the forcing $\overline{j}(\mathsf{M})_t$ depends on $\overline{\phi}_t$ and its neighbors. For the temporal ϕ^3 example, it takes the values tabulated in table 2.

Subtract (91) from (79) to obtain the 3-term recurrence for $\varphi_t = \phi_t - \overline{\phi}_t$, the deviations (89) from the shadow state,

$$-\varphi_{t+1} + 2\varphi_t - \varphi_{t-1} + \mu^2\left(-\phi_t^2 + \overline{\phi}_t^2\right) = \overline{j}(\mathsf{M})_t\,.$$

Substituting $\phi_t^2 = (\varphi_t + \overline{\phi}_t)^2$ and $j(\mathsf{M})_t = \overline{j}(\mathsf{M})_t + a\,\overline{\phi}_t^2$, we obtain

M-*forced Euler–Lagrange equation*

for the deviation φ_{M} from the shadow lattice state configuration $\overline{\Phi}_{\mathsf{M}}$:

$$-\varphi_{t+1} + 2\varphi_t - \varphi_{t-1} - \mu^2\left(\varphi_t + \overline{\phi}_t\right)^2 = j(\mathsf{M})_t\,. \tag{92}$$

[2024-02-15 Sidney] I still have to recompute the violation table table 2.

This is to be solved by whatever code you find optimal. For example:

Vattay inverse iteration (C.1) is now

$$\varphi_t^{(m+1)} = -\overline{\phi}_t + \sigma_t\frac{1}{\sqrt{a}}\left(j(\mathsf{M})_t + \varphi_{t+1}^{(m)} + \varphi_{t-1}^{(m)}\right)^{1/2}\,, \tag{93}$$

and that should converge like a ton of rocks.

Perhaps watch *Shadow state conspiracy* (35:26 min)

10.1. Primitive cell stability of a shadow periodic state

Comparing with the free field (**??**) orbit Jacobian matrix,

$$\mathcal{J}_{zz'} = -\Box_{zz'} \; + \; \mu^2 \delta_{zz'} \,,$$

the effective shadow state, site dependent Klein-Gordon masses in orbit Jacobian operators for ϕ^3 (58) are $\pm\mu^2$ (see (58), seems to conflict: check!), and for ϕ^4 (**??**) either μ^2 or $-2\mu^2$ (see (69)),

$$\overline{\mathcal{J}}_{zz'} = \; - \Box_{zz'} \; + \; \overline{\mu}_z^2 \, \delta_{zz'} \,, \quad \overline{\mu}_z^2 = m_z \mu^2 \,, \qquad\qquad m_z \in \{-1, 1\} \;, \tag{94}$$

$$\overline{\mathcal{J}}_{zz'} = \; - \Box_{zz'} \; + \; \overline{\mu}_z^2 \, \delta_{zz'} \,, \quad \overline{\mu}_z^2 = (1 \; - \; 3\,|m_z|)\, \mu^2, \; m_z \in \{-1, 0, 1\} \;. \tag{95}$$

In the anti-integrable, strong coupling regime, one can drop the Laplacian in $\mathrm{Det}\, \overline{\mathcal{J}}_p$, so the shadow Hill determinant is approximately the product of the above lattice-site dependent masses, and the shadow stability exponent is

$$\mathrm{Det}\, \overline{\mathcal{J}}_p = \prod_z^{\mathbb{A}} \overline{\mu}_z^2 \,, \qquad \overline{\lambda}_p = \frac{2}{N_{\mathbb{A}}} \sum_z^{\mathbb{A}} \ln |\overline{\mu}_z| \,, \tag{96}$$

so for ϕ^3 and spatiotemporal cat the anti-integrable limit of shadow stability exponent is periodic state-independent, simply $\overline{\lambda}_p = \ln \mu^2$, while for ϕ^4 theory $\overline{\lambda}_p$ depends on the number of '0's in periodic state's mosaic.

11. Symbol mosaic

In the theory of dynamical systems, symbolic dynamics is a powerful tool for systematically encoding distinct temporal orbits by their symbolic itineraries. Here we briefly review the symbolic dynamics for temporal dynamical systems, then generalize this method to spatiotemporal problems, where the symbol sequences are replaced by 'mosaics', d-dimensional symbols arrays, which represent spatiotemporal periodic states globally in the spacetime [43, 44, 55, 92, 93, 149, 150].

Mosaics represents orbits by arrays of letters from a finite alphabet. Count of admissible mosaics is a convenient way to count periodic states. Consider the map of ϕ^4 field theory as an example. In section 6.2 we show that the non-wandering set of the map is bounded and the map has a three-fold horseshoe, which intersects with the optimal cover of the non-wandering set in three separated regions. The non-wandering set in the state space can be partitioned by the three strips of the horseshoe, with each region labeled by a symbol in the three-letter alphabet $\{-1, 0, 1\}$. We choose the Klein-Gordon mass μ^2 large enough such that the horseshoe of the map is complete, so every symbol sequence corresponds to one periodic orbit of the system.

Given the symbol sequences, there are many different numerical methods that can find the corresponding periodic orbits, from the simplest Newton method, to more sophisticated approaches, such as Biham and Wenzel [27] method, Hansen [95] method, Vattay [53] 'inverse iteration' method and Sterling [197] 'anti-integrable continuation' method. All of these methods require a good initial starting point, so that they converge to the periodic orbit corresponding to the given symbol sequence. A good initial point can be constructed using the symbol sequence. For the map of ϕ^4 field theory with sufficiently large μ^2, using the pseudo-orbit consists of the fixed points corresponding to the symbols in the symbol sequence is already good enough to find the periodic orbit.

For spatiotemporal dynamical systems such as the spatiotemporal cat, spatiotemporal ϕ^3 and ϕ^4 field theory, the symbolic representation of periodic states can be given by symbol arrays, instead of symbol sequences. We refer to the symbol array as the *mosaic*. For a d-dimensional spatiotemporal system, the mosaic M_c of a periodic state Φ_c is a d-dimensional symbol array:

$$\mathsf{M}_c = \{m_z\} \,, \quad m_z \in \mathcal{A} \,, \quad z \in \mathbb{Z}^d \,, \tag{97}$$

where $\mathcal{A}$ is the alphabet of the symbols. Instead of treating the spatiotemporal systems as coupled maps and partitioning the high-dimensional state space, here we assign the global symbolic mosaics using the continuation from the anti-integrable limit of the systems, following the symbolic coding of Sterling *et al* [196–198] for coupled Hénon map lattice.

Consider the spatiotemporal ϕ^3 (48) and ϕ^4 (65) as examples. At the anti-integrable limit where the Klein-Gordon mass $\mu^2 \to \infty$, the ϕ^3 and ϕ^4 field theories are no longer deterministic. The temporal and spatial coupling becomes insignificant compare to the local potential, so the local field values do not depend on their neighbors, and the periodic states of the systems are arbitrary arrays of field values from a set of anti-integrable states, $\{-1/2, 1/2\}$ for ϕ^3 theory (48), and $\{-1, 0, 1\}$ for ϕ^4 theory (65). Using the set of the anti-integrable states as the symbolic alphabet $\mathcal{A}$, Sterling *et al* [196–198] showed that for single and coupled Hénon map, every symbol mosaic M_c corresponds to an unique periodic state Φ_c which is contained in a neighborhood of M_c, providing that the system is sufficiently close to the anti-integrable limit. Applying this symbolic coding to spatiotemporal ϕ^3 and ϕ^4 field theories, we have a 2-letter alphabet for ϕ^3 theory and a 3-letter alphabet for ϕ^4 theory. In this paper we choose sufficiently large Klein-Gordon mass μ^2 such that every symbol mosaic is admissible in our desired spatiotemporal domain. The mosaics are close to the corresponding periodic states, hence they are good initial starting points for numerically finding the periodic states.

12. Symmetry

All the chaotic field theories that we have examined in this and our companion papers [LC21,CL18] can be written as

$$-\Box\Phi + s[\Phi] = \mathbf{M} \tag{98}$$

Where $s[\Phi]$ changes depending on what theory we are using. This can, in turn, be written as matrix multiplication

$$(-\Box + \mathcal{J}[\Phi])\Phi = \mathbf{M} \tag{99}$$

Using the definition of a physical law being invariant

$$F(\Phi) = g^{-1}F(g\Phi) \tag{100}$$

By inspection, we know that $g^{-1}\Box g = \Box$ for all elements in C_∞ and D_∞, next we note that in the basis where all lattice states have been rotated or reflected by some element of D_∞ the appropriate orbit Jacobian is $\mathcal{J}[g\Phi]$ with this in mind, carrying through with (100) shows that the cat map, ϕ^3, and ϕ^4 are all invariant under D_∞. Realizing that our lattice equations have inherent symmetries is extremely useful. We can utilize them to speed up calculations, and make deeper theoretical observations...as long as we understand the symmetries we are working with.

12.1. Symmetries of the square lattice

[2023-03-04 Predrag] Will redraw figure 5 as 3 horizontal frames, once we are finalizing the paper.
A prime periodic state usually has less symmetry than D_4 / *p4mm* [63]. Mapped back into the unit square, its point group will be one of the square lattice point groups in the wallpaper classification.

[2023-05-06 Predrag] As long as we study translations only. Once there are discrete symmetries, smaller prime periodic states might be demanded by the discrete symmetry.

The unit cell of the integer lattice (**??**) tiles a hypercubic lattice under action of d commuting translations (**??**), called 'shifts' for infinite lattices, 'rotations' for finite periodic lattices. They form the abelian *translation group* $T = \{r_j^k \,|\, j = 1, 2, \cdots, d\,, \;\; k \in \mathbb{Z}\}$, where $r_j^0 = \mathbb{1}_j$ denotes the identity, and r_j, r_j^2, $\cdots$, r_j^k, $\cdots$, denote translations by $1, 2, \cdots, k, \cdots$ lattice sites in the jth spatiotemporal direction. For a square lattice, the translation group consists of the product of two commuting infinite cyclic groups $T = \mathrm{C}_{\infty,1} \otimes \mathrm{C}_{\infty,2}$, with

$$\mathrm{C}_{\infty,j} = \{\cdots, r_j^{-2}, r_j^{-1}, \mathbb{1}, r_j^1, r_j^2, r_j^3, \cdots\} \tag{101}$$

in the jth direction.

For space groups, the cosets by translation subgroup T form the *factor* (also known as *quotient*) group G/T, isomorphic to the point group g.

The Euler–Lagrange equations that define the spatiotemporal lattice field theories of section **??** are invariant under the discrete spacetime translations; the space σ_1 and time σ_3 reflections $n \to -n$, $t \to -t$; as well as under σ and σ_2 exchanges $n \longleftrightarrow t$ of space and time. They thus have the point-group symmetries of the square lattice: rotation C by $\pi/2$, reflections σ_1 across space-axis, σ_3 across time-axis, and σ_0, σ_2 across the two spacetime diagonals,

$$\mathrm{D}_4 = \{e, C, C^2, C^4, \sigma_1, \sigma_3, \sigma_0, \sigma_2\}\,, \tag{102}$$

see figure 5. In the international crystallographic notation, this square lattice space group of symmetries is referred to as *p4mm* [63].

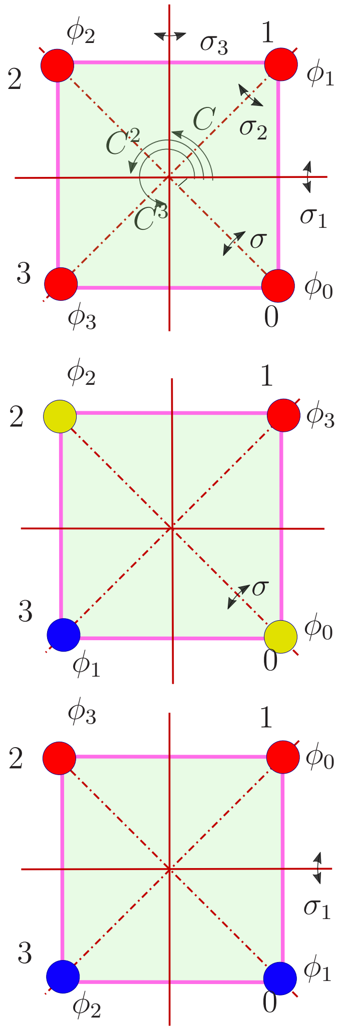

Figure 5: (Color online) Dihedral group D_4, the group of all symmetries (102) that overlie a square onto itself, consists of 3 rotations C^k that permute the sites cyclically, and 4 rotate-reflect elements σ_k that reflect the square across reflection axes, exchanging the red and the blue sites. An even reflection (long diagonal, dashed line reflection axis), here σ, leaves a pair of opposite sites fixed (marked yellow), while an odd reflection axis (short diagonal, full line), here σ_1, bisects the opposite edges, and flips all sites.

Classifying periodic states by their factor group G/T is already not a simple undertaking in one temporal dimension (the subject of paper I), where it amounts to a purely group-theoretic reduction of the time reversal symmetry. While D_4 is the point group (102) of the unit square, each Bravais lattice (**??**) has its own factor group G/T, and -for purposes of this exposition- classifying them would lead us far from our main thrust. Here we shall construct the partition function and its reciprocal lattice representation in terms of prime periodic states, assuming only the $T = C_{\infty,1} \otimes C_{\infty,2}$ space and time translational invariance of system's Euler–Lagrange equations. The cost of ignoring the point-group symmetries is overcounting reflection-symmetric periodic states.

12.2. Internal symmetries

In addition to section 12.1 spacetime 'geometrical' symmetries: invariance of the shape of a periodic state under coordinate translations, rotations, and reflections, a field theory might have *internal* symmetries, groups of transformations that leave the Euler–Lagrange equations invariant, but act only on a lattice site *field*, not on site's location in the spacetime lattice.

For example, the ϕ^4 Euler–Lagrange equation (12) is invariant under the D_1 reflection $\phi_z \to -\phi_z$, and the spatiotemporal cat (10) is invariant under D_1 inversion of the field though the center of the $0 \leq \phi_z < 1$ unit interval:

$$\bar{\phi}_z = 1 - \phi_z \mod 1 \,, \qquad \text{for all } j \in \mathcal{L} \,, \tag{103}$$

and the corresponding inversion of lattice site symbol m_z. If $\Phi = \{\phi_z\}$ is a periodic state of the system, its inversion $\bar{\Phi} = \{\bar{\phi}_z\}$ is also a periodic state. So every periodic state of either belongs to a pair of asymmetric periodic states $\{\Phi, \bar{\Phi}\}$, or is symmetric under the inversion.

In principle, the internal symmetries should also be taken care of, but to keep the exposition simple, they are not quotiented in this paper.

12.3. What are 'periodic states'? Orbits?

[2023-08-26 Predrag] Currently this section is full clip&paste from LC21 [137]. Adopt it to the needs of this paper.

For evolution-in-time, every period-n periodic point is a fixed point of the nth iterate of the 1 time-step map. In the lattice formulation, the totality of finite-period periodic states is the *set of fixed points* of all $H_{\mathbf{a}}$ and $H_{\mathbf{a},k}$ subgroups of D_∞.

Definition: Orbit *or* G-orbit *of a periodic state* Φ *is the set of all periodic states*

$$\mathcal{M}_\Phi = \{g\,\Phi \mid g \in G\} \tag{104}$$

into which Φ *is mapped under the action of group* G*. We label the orbit* $\mathcal{M}_\Phi$ *by any periodic state* Φ *belonging to it.*

Definition: Symmetry of a solution. *We shall refer to the maximal subgroup* $G_\Phi \subseteq G$ *of actions which permute periodic states within the orbit* $\mathcal{M}_\Phi$*, but leave the orbit invariant, as the* symmetry G_Φ *of the orbit* $\mathcal{M}_\Phi$*,*

$$G_\Phi = \{g \in G_\Phi \mid g\mathcal{M}_\Phi = \mathcal{M}_\Phi\} \,. \tag{105}$$

An orbit $\mathcal{M}_\Phi$ is G_Φ-*symmetric* (*symmetric*, *set-wise symmetric*, *self-dual*) if the action of elements of G_Φ on the set of periodic states $\mathcal{M}_\Phi$ reproduces the orbit.

Definition: Index *of orbit* $\mathcal{M}_\Phi$ *is given by*

$$m_\Phi = |G|/|G_\Phi| \tag{106}$$

(see Wikipedia [213] and Dummit and Foote [68]).

And now, a pleasant surprise, obvious upon an inspection of figures **??** and **??**: what happens in the primitive cell, stays in the primitive cell. Even though the lattices $\mathcal{L}$, $\mathcal{L}_\mathbf{a}$ are infinite, and their symmetries D_∞, $H_\mathbf{a}$, $H_{\mathbf{a},k}$ are *infinite* groups, the Bravais periodic states' *orbits* are *finite*, described by the finite group permutations of the infinite lattice curled up into a primitive cell periodic n-site ring.

13. Summary

How to think about matters spatiotemporal?

Acknowledgments

We are grateful to [...] . No actual cats, graduate or undergraduate were harmed during this research.

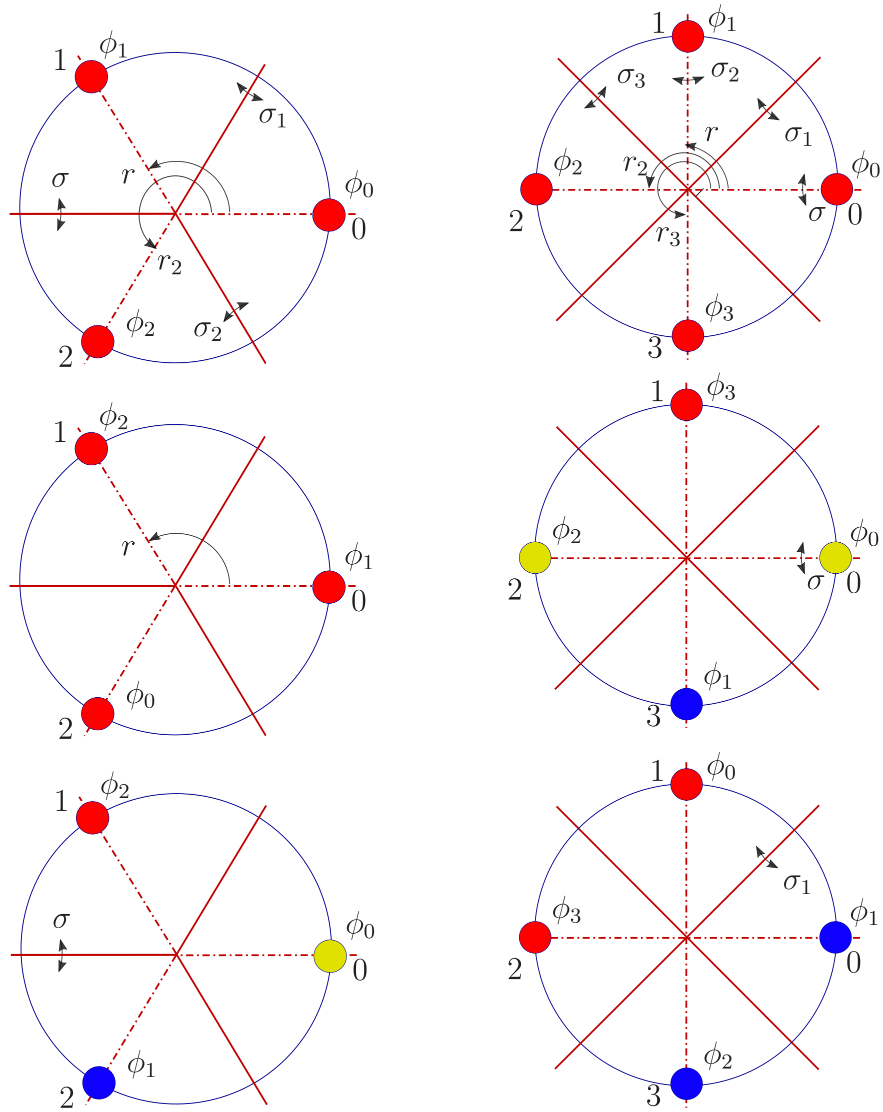

Figure 6: (Color online) Consider a period-n primitive cell tiling of a one-dimensional lattice $\mathcal{L}$. With $\mathcal{L}$ curled into a ring of n lattice sites, actions of the infinite dihedral group D_∞ reduce to translational and reflection symmetries of (D$_3$) an equilateral triangle, $n = 3$ lattice sites; (D$_4$) a square, $n = 4$ lattice sites; all group operations that overlie an n-sided regular polygon onto itself. The n translations r_j permute the sites cyclically. The n dihedral group D_n translate-reflect σ_k elements (**??**) reflect the sites across reflection axes, exchanging red and blue sites. For even n, an even reflection (dashed line reflection axis), here σ, leaves a pair of opposite sites fixed (marked yellow), while an odd reflection axis (full line), here σ_1, bisects the opposite edges, and flips all sites. For odd n, every reflection half-axis leaves a site fixed (dashed line), and bisects the opposite edge (full line). This periodic ring visualization makes it obvious that any symmetric periodic state is reflection invariant across two points on the lattice, see figure **??**.

Appendix A. Spatiotemporal Hénon

[2024-03-06 Predrag] Move to here all Hénon text previously in the Tigers' `phi3.tex`

The simplest nonlinear field theory with polynomial potential, the scalar ϕ^3 theory, turns out to be the spacetime generalization of the paradigmatic dynamicist's model of a two-dimensional nonlinear dynamical system, the quadratic Hénon map [99]

$$\begin{aligned} x_{t+1} &= 1 - a\,x_t^2 + b\,y_t \\ y_{t+1} &= x_t\,. \end{aligned} \tag{A.1}$$

For the contraction parameter value $b = -1$ this is an area-preserving, Hamiltonian map. The Hénon map is the simplest map that captures chaos that arises from the smooth stretch & fold dynamics of nonlinear return maps of flows such as Rössler [184].

The map can be interpreted as a kicked driven anaharmonic oscillator [98], with the nonlinear, cubic Biham-Wenzel [27] lattice site potential (27)

$$V(\phi) = \frac{1}{2}\,\mu^2\phi^2 - \frac{1}{3!}\,g\,\phi^3\,, \tag{A.2}$$

so we refer to this field theory as ϕ^3 theory. A parameter can be rescaled away by translations and rescalings of the field ϕ, and the Euler–Lagrange equation of the system can brought to various equivalent forms, such as the Hénon form (A.3), or the anti-integrable form (A.4),

Written as a 2nd-order inhomogeneous difference equation [67], (A.1) takes the nearest-neighbor Laplacian form, the Euler–Lagrange equation (8),

$$-\,\Box\varphi_z + a\,\varphi_z^2 - 2d\,\varphi_z + 1 = 0\,. \tag{A.3}$$

To bring this to a form more convenient for our purposes, complete the square,

$$-\,\Box\varphi_z - a\left[\left(\varphi_z + \frac{d}{a}\right)^2 - \frac{d^2+a}{a^2}\right] = 0\,,$$

and rescale the field as $\varphi = -A\phi$,

$$-\,\Box\phi_z - aA\left[\left(\phi_z + \frac{d}{aA}\right)^2 - \frac{d^2+a}{(aA)^2}\right] = 0\,.$$

To cast this into the anti-integrable form pick a convenient set of roots, for example the symmetric pair $(1/2, -1/2)$, separated by 1. Then $(aA)^2 = 4(a+d^2)$. Calling that parameter the 'Klein-Gordon mass squared' μ^2, the Euler–Lagrange equation takes the anti-integrable form, with the potential dominating for large μ^2,

$$-\,\Box\phi_z \;+\; \mu^2\,(1/4 - \phi_z^2) = 0\,. \tag{A.4}$$

To compare our results with the extensive, single temporal dimension, we note that the Hénon stretching parameter a in (A.3) and the Klein-Gordon mass μ^2 in (A.4) are related by

$$\mu^2 = 2\sqrt{a+1}\,. \tag{A.5}$$

For a sufficiently large 'stretching parameter' a, or 'mass parameter' μ^2, the periodic states of this ϕ^3 theory are in one-to-one correspondence to the unimodal Hénon map Smale horseshoe repeller, cleanly split into the 'left', positive stretching and 'right', negative stretching lattice site field values. A plot of such horseshoe, given in, for example, ChaosBook Example 15.4, is helpfull in understanding that state space of deterministic solutions of strongly nonlinear field theories has fractal support. Devaney, Nitecki, Sterling and Meiss [59, 196, 198] have shown that the Hamiltonian Hénon map has a complete Smale horseshoe for stretching parameter a or Klein-Gordon mass μ^2 values (A.5) above

$$a > 5.699310786700\cdots\ . \tag{A.6}$$

$$\mu^2 > 5.17660536904\cdots\ . \tag{A.7}$$

In numerical [53] and analytic [72] calculations ChaosBook fixes the stretching parameter value to $a = 6$, $\mu^2 = 5.29150262213$, in order to guarantee that all 2^n periodic points $\phi = f^n(\phi)$ of the Hénon map (A.1) exist.

[2024-03-06 Predrag] Why not use $\mu^2 = 5.2$?

The symbolic dynamics is binary.

[2023-08-01 Predrag] Politi and Torcini [174] study of periodic states of spatiotemporal Hénon, a (1+1)-spacetime lattice of Hénon maps with solutions periodic both in space and time is the closest to the present investigation. They explain why the dependence of the lattice field at time ϕ_{t+1} on the two previous time steps prevents an interpretation of dynamics as the composition of a local chaotic evolution with a diffusion process. In the CML tradition, they study the weak coupling regime $\epsilon \approx 0$.

[2023-10-28 Predrag] A ϕ^3 paper for Tigers to check: Knill writes in QuantumCalculus.org: "looked at coupled standard maps which emerged when looking at extremization problems of Wilson type. The paper was called "Nonlinear dynamics from the Wilson Lagrangian". It is quite a neat variational problem to maximize the functional $\mathrm{tr}((D+im)^4)$ on some space of operators, where m is a mass parameter. This naturally leads in the simplest case to Hénon type cubic symplectic maps and in higher dimensions to coupled map lattices where one can prove the existence of bounded solutions using the anti-integrable limit of Aubry. "

Appendix B. Inverse iteration method

(Gábor Vattay, Sidney V. Williams and P. Cvitanović)

The 'inverse iteration method' for determining the periodic orbits of 2-dimensional repeller was introduced by G. Vattay as a ChaosBook.org *Inverse iteration method for a Hénon repeller*. (See also the solution on page **??**.) The idea of the method is to ⇓PRIVATE ⇑PRIVATE

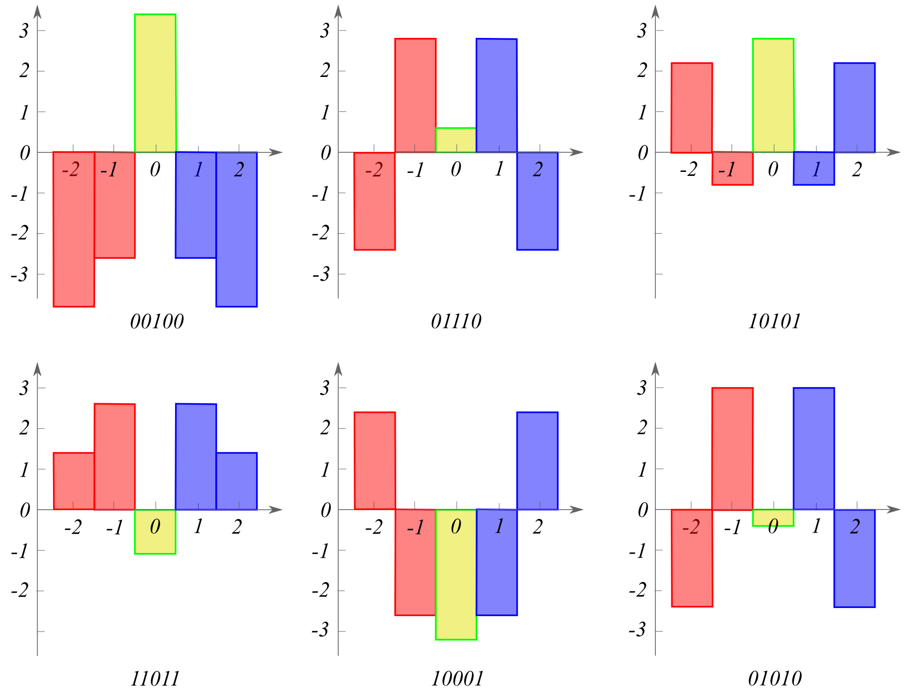

Figure A1: Temporal Hénon (**??**), $a = 6$: All period $n = 5$ prime periodic states $\overline{\phi_{-2}\phi_{-1}\boxed{\phi_0}\phi_1\phi_2|}$ of table **??**. They are all reflection symmetric, with the fixed lattice field $\boxed{\phi_0}$ colored gold. The most striking feature is how far the $a = 6$ temporal Hénon is from the $0 \leftrightarrow 1$ symmetry: stretching close to $\overline{0}$ fixed point periodic state is much stronger than close to the almost marginal $\overline{1}$ fixed point periodic state. For a stretching parameter value a slight lower than the critical value $a_h = 5.69931\cdots$, the lattice sites $\boxed{\phi_0}$ for $\overline{01110}$ and $\overline{01010}$ coalesce and vanish through an inverse bifurcation. As $a \to \infty$ we expect this symmetry to be restored.

(1) Guess a lattice configuration $\phi_t^{(0)}$ that qualitatively looks like the desired periodic state. For that, you need a qualitative, symbolic dynamics description of system's admissible periodic states. You can get started by a peak at ChaosBook Table 18.1.

(2) Compare the 'stretched' field $\phi_t^{(0)}$ to its neighbors, using system's defining equation. For example, ϕ^3 (or temporal Hénon) Euler–Lagrange equation (49) is

$$-\phi_{t+1} - \left(\mu^2\,\phi_t^2 - 2\,\phi_t + \frac{\mu^2}{4}\right) - \phi_{t-1} \;=\; 0\,.$$

Perhaps watch *What's "The Law"?* (4 min).

(3) Use the amount by which ϕ_t 'sticks out' in violation of the defining equations to obtain a better value $\phi_t^{(1)}$, for every lattice site t. Vattay does that by inverting the equation, determining $\phi_t^{(1)}$ from its neighbors

$$\phi_t^{(m+1)} = \sigma_t \frac{1}{\sqrt{a}}\left(1 + \phi_{t+1}^{(m)} + \phi_{t-1}^{(m)}\right)^{1/2} \tag{B.1}$$

where σ_t is the sign of the target site field $\sigma_t = \phi_t/|\phi_t|$, prescribed in advance by specifying the desired Hénon symbol block

$$\sigma_t = 1 - 2\, m_t\,, \quad m_t \in \{0,1\}\,. \tag{B.2}$$

Perhaps watch *Inverse iteration method* (14:28 min).

(4) Wash and repeat, $\phi_t^{(m)} \to \phi_t^{(m+1)}$. Sidney starts the iteration by setting the initial guess lattice site fields to

$$\phi_t^{(0)} = \sigma_t/\sqrt{a}\,,$$

and then loops (C.1) through all lattice site fields to obtain $\phi_t^{(1)}$. When $|\phi_t^{(m+1)} - \phi_t^{(1)}|$ for all periodic states is smaller than a desired tolerance, the loop terminates, and the periodic state is found. An example of the resulting periodic states is given in figure A1.

The meat of the method is contained in these two loops:

```
for i in range(0,len(symbols)):
cycle[i]=signs[i]*np.sqrt(abs(1-np.roll(cycle,1)[i]-np.roll(cycle,-1)[i])/a)
for i in range(0,len(symbols)):
deviation[i]=np.roll(cycle,-1)[i]-(1-a*(cycle[i])**2-np.roll(cycle,1)[i])
```

The method applies to strongly coupled ϕ^3 field theory in any spatiotemporal dimension. For example, in 2 spacetime dimensions, the mth inverse iterate (C.1) compares the 'stretched' field $\phi_{nt}^{(0)}$ to its 4 neighbors,

$$\phi_{nt}^{(m+1)} = \sigma_{nt} \frac{1}{\sqrt{2a}} \left(2 + \phi_{n,t+1}^{(m)} + \phi_{n,t-1}^{(m)} + \phi_{n+1,t}^{(m)} + \phi_{n-1,t}^{(m)}\right)^{1/2}\,. \tag{B.3}$$

It is applied to each of the LT lattice site fields $\{\phi_{nt}^{(m)}\}$ of a doubly periodic primitive cell $[L\times T]_S$. Here σ_{nt} is the sign of the target site field $\sigma_{nt} = \phi_{nt}/|\phi_{nt}|$, prescribed in advance by specifying the desired Hénon symbol block M,

$$\sigma_{nt} = 1 - 2\, m_{nt}\,, \quad m_{nt} \in \{0,1\}\,. \tag{B.4}$$

For the *temporal Hénon* 3-term recurrence (**??**), the system's state space Smale horseshoe is again generated by iterates of the region plotted in figure 4. So, positive field ϕ_{nt} value has $m_{nt} = 0$, negative field ϕ_{nt} value has $m_{nt} = 1$.

Appendix C. Inverse iteration method

(Gábor Vattay, Sidney V. Williams and P. Cvitanović)

The 'inverse iteration method' for determining the periodic orbits of 2-dimensional repeller was introduced by G. Vattay as a ChaosBook.org *Inverse iteration method for a Hénon repeller.* (See also the solution on page **??**.) The idea of the method is to

⇓PRIVATE
⇑PRIVATE

(1) Guess a lattice configuration $\phi_t^{(0)}$ that qualitatively looks like the desired periodic state. For that, you need a qualitative, symbolic dynamics description of system's admissible periodic states. You can get started by a peak at ChaosBook Table 18.1.

(2) Compare the 'stretched' field $\phi_t^{(0)}$ to its neighbors, using system's defining equation. For example, ϕ^3 (or temporal Hénon) Euler–Lagrange equation (49) is

$$-\phi_{t+1} - \left(\mu^2\,\phi_t^2 - 2\,\phi_t + \frac{\mu^2}{4}\right) - \phi_{t-1} \;=\; 0\,.$$

Perhaps watch *What's "The Law"?* (4 min).

(3) Use the amount by which ϕ_t 'sticks out' in violation of the defining equations to obtain a better value $\phi_t^{(1)}$, for every lattice site t. Vattay does that by inverting the equation, determining $\phi_t^{(1)}$ from its neighbors

$$\phi_t^{(m+1)} = \sigma_t \frac{1}{\sqrt{a}} \left(1 + \phi_{t+1}^{(m)} + \phi_{t-1}^{(m)}\right)^{1/2} \tag{C.1}$$

where σ_t is the sign of the target site field $\sigma_t = \phi_t/|\phi_t|$, prescribed in advance by specifying the desired Hénon symbol block

$$\sigma_t = 1 - 2\,m_t\,, \quad m_t \in \{0, 1\}\,. \tag{C.2}$$

Perhaps watch *Inverse iteration method* (14:28 min).

(4) Wash and repeat, $\phi_t^{(m)} \to \phi_t^{(m+1)}$. Sidney starts the iteration by setting the initial guess lattice site fields to

$$\phi_t^{(0)} = \sigma_t/\sqrt{a}\,,$$

and then loops (C.1) through all lattice site fields to obtain $\phi_t^{(1)}$. When $|\phi_t^{(m+1)} - \phi_t^{(1)}|$ for all periodic states is smaller than a desired tolerance, the loop terminates, and the periodic state is found. An example of the resulting periodic states is given in figure A1.

The meat of the method is contained in these two loops:

```
for i in range(0,len(symbols)):
cycle[i]=signs[i]*np.sqrt(abs(1-np.roll(cycle,1)[i]-np.roll(cycle,-1)[i])/a)
for i in range(0,len(symbols)):
deviation[i]=np.roll(cycle,-1)[i]-(1-a*(cycle[i])**2-np.roll(cycle,1)[i])
```

The method applies to strongly coupled ϕ^3 field theory in any spatiotemporal dimension. For example, in 2 spacetime dimensions, the mth inverse iterate (C.1) compares the 'stretched' field $\phi_{nt}^{(0)}$ to its 4 neighbors,

$$\phi_{nt}^{(m+1)} = \sigma_{nt} \frac{1}{\sqrt{2a}} \left(2 + \phi_{n,t+1}^{(m)} + \phi_{n,t-1}^{(m)} + \phi_{n+1,t}^{(m)} + \phi_{n-1,t}^{(m)}\right)^{1/2}\,. \tag{C.3}$$

It is applied to each of the LT lattice site fields $\{\phi_{nt}^{(m)}\}$ of a doubly periodic primitive cell $[L\times T]_S$. Here σ_{nt} is the sign of the target site field $\sigma_{nt} = \phi_{nt}/|\phi_{nt}|$, prescribed in advance by specifying the desired Hénon symbol block M,

$$\sigma_{nt} = 1 - 2\,m_{nt}\,, \quad m_{nt} \in \{0, 1\}\,. \tag{C.4}$$

For the *temporal Hénon* 3-term recurrence (**??**), the system's state space Smale horseshoe is again generated by iterates of the region plotted in figure 4. So, positive field ϕ_{nt} value has $m_{nt} = 0$, negative field ϕ_{nt} value has $m_{nt} = 1$.

References

[1] M. Akila, B. Gutkin, P. Braun, D. Waltner, and T. Guhr, "Semiclassical prediction of large spectral fluctuations in interacting kicked spin chains", Ann. Phys. **389**, 250–282 (2018).

[2] M. Akila, D. Waltner, B. Gutkin, P. Braun, and T. Guhr, "Semiclassical identification of periodic orbits in a quantum many-body system", Phys. Rev. Lett. **118**, 164101 (2017).

[3] M. Akila, D. Waltner, B. Gutkin, and T. Guhr, "Particle-time duality in the kicked Ising spin chain", J. Phys. A **49**, 375101 (2016).

[4] V. V. Albert, L. I. Glazman, and L. Jiang, "Topological properties of linear circuit lattices", Phys. Rev. Lett. **114**, 173902 (2015).

[5] E. Allroth, "Ground state of one-dimensional systems and fixed points of 2n-dimensional map", J. Phys. A **16**, L497 (1983).

[6] R. E. Amritkar, P. M. Gade, A. D. Gangal, and V. M. Nandkumaran, "Stability of periodic orbits of coupled-map lattices", Phys. Rev. A **44**, R3407–R3410 (1991).

[7] S. Anastassiou, A. Bountis, and A. Bäcker, "Homoclinic points of 2D and 4D maps via the parametrization method", Nonlinearity **30**, 3799–3820 (2017).

[8] W. N. Anderson and T. D. Morley, "Eigenvalues of the Laplacian of a graph", Lin. Multilin. Algebra **18**, 141–145 (1985).

[9] F. Arrigo, P. Grindrod, D. J. Higham, and V. Noferini, "On the exponential generating function for non-backtracking walks", Linear Algebra Appl. **556**, 381–399 (2018).

[10] J. H. Asad, "Differential equation approach for one- and two-dimensional lattice green's function", Mod. Phys. Lett. B **21**, 139–154 (2007).

[11] D. Atkinson and F. J. van Steenwijk, "Infinite resistive lattices", Am. J. Phys **67**, 486–492 (1999).

[12] S. Aubry, "Anti-integrability in dynamical and variational problems", Physica D **86**, 284–296 (1995).

[13] S. Aubry and G. Abramovici, "Chaotic trajectories in the standard map. The concept of anti-integrability", Physica D **43**, 199–219 (1990).

[14] M. Baake, J. Hermisson, and A. B. Pleasants, "The torus parametrization of quasiperiodic LI-classes", J. Phys. A **30**, 3029–3056 (1997).

[15] J.-C. Ban, W.-G. Hu, S.-S. Lin, and Y.-H. Lin, *Zeta Functions for Two-dimensional Shifts of Finite Type*, Vol. 221, Memoirs Amer. Math. Soc. (Amer. Math. Soc., Providence RI, 2013).

[16] R. Band, J. M. Harrison, and C. H. Joyner, "Finite pseudo orbit expansions for spectral quantities of quantum graphs", J. Phys. A **45**, 325204 (2012).

[17] A. Barvinok, *A Course in Convexity* (Amer. Math. Soc., New York, 2002).

[18] A. Barvinok, *Integer Points in Polyhedra* (European Math. Soc. Pub., Berlin, 2008).

[19] H. Bass, "The Ihara-Selberg zeta function of a tree lattice", Int. J. Math. **3**, 717–797 (1992).

[20] R. J. Baxter, "The bulk, surface and corner free energies of the square lattice Ising model", J. Phys. A **50**, 014001 (2016).

[21] M. Beck and S. Robins, *Computing the Continuous Discretely* (Springer, New York, 2007).

[22] B. Bertini, P. Kos, and T. Prosen, "Exact spectral form factor in a minimal model of many-body quantum chaos", Phys. Rev. Lett. **121**, 264101 (2018).

[23] B. Bertini, P. Kos, and T. Prosen, "Entanglement spreading in a minimal model of maximal many-body quantum chaos", Phys. Rev. X **9**, 021033 (2019).

[24] B. Bertini, P. Kos, and T. Prosen, "Exact correlation functions for dual-unitary lattice models in 1+1 dimensions", Phys. Rev. Lett. **123**, 210601 (2019).

[25] B. Bertini, P. Kos, and T. Prosen, "Operator entanglement in local quantum circuits i: Chaotic dual-unitary circuits", SciPost Physics **8**, 067 (2020).

[26] H. S. Bhat and B. Osting, "Diffraction on the two-dimensional square lattice", SIAM J. Appl. Math. **70**, 1389–1406 (2010).

[27] O. Biham and W. Wenzel, "Characterization of unstable periodic orbits in chaotic attractors and repellers", Phys. Rev. Lett. **63**, 819 (1989).

[28] P. Blanchard and D. Volchenkov, *Random Walks and Diffusions on Graphs and Databases* (Springer, Berlin, 2011).

[29] S. V. Bolotin and D. V. Treschev, "Hill's formula", Russ. Math. Surv. **65**, 191 (2010).

[30] T. Bountis and R. H. G. Helleman, "On the stability of periodic orbits of two-dimensional mappings", J. Math. Phys **22**, 1867–1877 (1981).

[31] R. Bowen, "Markov partitions for Axiom A diffeomorphisms", Amer. J. Math. **92**, 725–747 (1970).

[32] R. Bowen and O. Lanford, Zeta functions of restrictions of the shift transformation, in Global Analysis (Proc. Sympos. Pure Math., Berkeley, CA, 1968), Vol. 1, edited by S.-S. Chern and S. Smale (1970), pp. 43–50.

[33] A. Boyarsky and P. Góra, *Laws of Chaos: Invariant Measures and Dynamical Systems in One Dimension* (Birkhäuser, Boston, 1997).

[34] L. Boyle and P. J. Steinhardt, Self-similar one-dimensional quasilattices, 2016.

[35] R. B. S. Brooks, R. F. Brown, J. Pak, and D. H. Taylor, "Nielsen numbers of maps of tori", Proc. Amer. Math. Soc. **52**, 398–398 (1975).

[36] A. Brown, "Equations for periodic solutions of a logistic difference equation", J. Austral. Math. Soc. Ser. B **23**, 78–94 (1981).

[37] B. L. Buzbee, G. H. Golub, and C. W. Nielson, "On direct methods for solving Poisson's equations", SIAM J. Numer. Anal. **7**, 627–656 (1970).

[38] J. L. Cardy, "Operator content of two-dimensional conformally invariant theories", Nucl. Phys. B **270**, 186–204 (1986).

[39] M. Cencini, A. Puglisi, D. Vergni, and A. Vulpiani, *A Random Walk in Physics* (Springer, 2021).

[40] M. Chen, "On the solution of circulant linear systems", SIAM J. Numer. Anal. **24**, 668–683 (1987).

[41] G. Chinta, J. Jorgenson, and A. Karlsson, "Zeta functions, heat kernels, and spectral asymptotics on degenerating families of discrete tori", Nagoya Math. J. **198**, 121–172 (2010).

[42] G. Chinta, J. Jorgenson, and A. Karlsson, "Heat kernels on regular graphs and generalized Ihara zeta function formulas", Monatsh. Math. **178**, 171–190 (2014).

[43] S.-N. Chow, J. Mallet-Paret, and W. Shen, "Traveling waves in lattice dynamical systems", J. Diff. Equ. **149**, 248–291 (1998).

[44] S.-N. Chow, J. Mallet-Paret, and E. S. Van Vleck, "Pattern formation and spatial chaos in spatially discrete evolution equations", Random Comput. Dynam. **4**, 109–178 (1996).

[45] F. Chung and S.-T. Yau, "Discrete Green's functions", J. Combin. Theory A **91**, 19–214 (2000).

[46] D. Cimasoni, "The critical Ising model via Kac-Ward matrices", Commun. Math. Phys. **316**, 99–126 (2012).

[47] B. Clair, "The Ihara zeta function of the infinite grid", Electron. J. Combin. **21**, P2–16 (2014).

[48] B. Clair and S. Mokhtari-Sharghi, "Zeta functions of discrete groups acting on trees", J. Algebra **237**, 591–620 (2001).

[49] B. Clair and S. Mokhtari-Sharghi, "Convergence of zeta functions of graphs", Proc. Amer. Math. Soc. **130**, 1881–1887 (2002).

[50] H. Cohen, *A Course in Computational Algebraic Number Theory* (Springer, Berlin, 1993).

[51] J. Cserti, "Application of the lattice Green's function for calculating the resistance of an infinite network of resistors", Amer. J. Physics **68**, 896–906 (2000).

[52] J. Cserti, G. Széchenyi, and G. Dávid, "Uniform tiling with electrical resistors", J. Phys. A **44**, 215201 (2011).

[53] P. Cvitanović, R. Artuso, R. Mainieri, G. Tanner, and G. Vattay, *Chaos: Classical and Quantum* (Niels Bohr Inst., Copenhagen, 2023).

[54] P. Cvitanović, R. Artuso, L. Rondoni, and E. A. Spiegel, "Transporting densities", in *Chaos: Classical and Quantum*, edited by P. Cvitanović, R. Artuso, R. Mainieri, G. Tanner, and G. Vattay (Niels Bohr Inst., Copenhagen, 2023).

[55] P. Cvitanović and H. Liang, A chaotic lattice field theory in two dimensions, In preparation, 2023.

[56] F. Dannan, S. Elaydi, and P. Liu, "Periodic solutions of difference equations", J. Difference Equations and Applications **6**, 203–232 (2000).

[57] J. A. De Loera, R. Hemmecke, J. Tauzer, and R. Yoshida, "Effective lattice point counting in rational convex polytopes", J. Symbolic Comp. **38**, 1273–1302 (2004).

[58] A. Deitmar, "Ihara zeta functions of infinite weighted graphs", SIAM J. Discrete Math. **29**, 2100–2116 (2015).

[59] R. L. Devaney and Z. Nitecki, "Shift automorphisms in the Hénon mapping", Commun. Math. Phys. **67**, 137–146 (1979).

[60] A. Dienstfrey, F. Hang, and J. Huang, "Lattice sums and the two-dimensional, periodic Green's function for the Helmholtz equation", Proc. Roy. Soc. Ser A **457**, 67–85 (2001).

[61] F. W. Dorr, "The direct solution of the discrete Poisson equation on a rectangle", SIAM Rev. **12**, 248–263 (1970).

[62] P. G. Doyle and J. L. Snell, "Random walks and electric networks", in *Intelligent Systems, Control and Automation: Science and Engineering* (Springer, 2012), pp. 259–265.

[63] M. S. Dresselhaus, G. Dresselhaus, and A. Jorio, *Group Theory: Application to the Physics of Condensed Matter* (Springer, New York, 2007).

[64] D. J. Driebe, *Fully Chaotic Maps and Broken Time Symmetry* (Springer, New York, 1999).

[65] J. Dubout, Zeta functions of graphs, their symmetries and extended Catalan numbers.

[66] D. Dudgeon and R. M. Mersereau, *Multidimensional Digital Signal Processing* (Prentice-Hall, Englewood Cliffs, NJ, 1984).

[67] H. R. Dullin and J. D. Meiss, "Generalized Hénon maps: the cubic diffeomorphisms of the plane", Physica D **143**, 262–289 (2000).

[68] D. S. Dummit and R. M. Foote, *Abstract Algebra* (Wiley, 2003).

[69] E. N. Economou, *Green's Functions in Quantum Physics* (Springer, Berlin, 2006).

[70] S. Elaydi, *An Introduction to Difference Equations*, 3rd ed. (Springer, Berlin, 2005).

[71] A. Endler and J. A. C. Gallas, "Conjugacy classes and chiral doublets in the Hénon Hamiltonian repeller", Phys. Lett. A **356**, 1–7 (2006).

[72] A. Endler and J. A. C. Gallas, "Reductions and simplifications of orbital sums in a Hamiltonian repeller", Phys. Lett. A **352**, 124–128 (2006).

[73] T. Engl, J. Dujardin, A. Argüelles, P. Schlagheck, K. Richter, and J. D. Urbina, "Coherent backscattering in Fock space: A signature of quantum many-body interference in interacting bosonic systems", Phys. Rev. Lett. **112**, 140403 (2014).

[74] T. Engl, P. Plöss, J. D. Urbina, and K. Richter, "The semiclassical propagator in fermionic Fock space", Theor. Chem. Acc. **133**, 1563 (2014).

[75] T. Engl, J. D. Urbina, Q. Hummel, and K. Richter, "Complex scattering as canonical transformation: A semiclassical approach in Fock space", Ann. Phys. **527**, 737–747 (2015).

[76] T. Engl, J. D. Urbina, and K. Richter, "Periodic mean-field solutions and the spectra of discrete bosonic fields: Trace formula for Bose-Hubbard models", Phys. Rev. E **92**, 062907 (2015).

[77] T. Engl, J. D. Urbina, and K. Richter, "The semiclassical propagator in Fock space: dynamical echo and many-body interference", Philos. Trans. Royal Soc. A **374**, 20150159 (2016).

[78] A. L. Fetter and J. D. Walecka, *Theoretical Mechanics of Particles and Continua* (Dover, New York, 2003).

[79] M. Fiedler, "Algebraic connectivity of graphs", Czech. Math. J **23**, 298–305 (1973).

[80] D. Fischer, G. Golub, O. Hald, C. Leiva, and O. Widlund, "On Fourier-Toeplitz methods for separable elliptic problems", Math. Comput. **28**, 349–349 (1974).

[81] L. Flatto, J. C. Lagarias, and B. Poonen, "The zeta function of the beta transformation", Ergodic Theory Dynam. Systems **14**, 237–266 (1994).

[82] F. Flicker, "Time quasilattices in dissipative dynamical systems", SciPost Phys. **5**, 001 (2018).

[83] E. Fradkin, *Field Theories of Condensed Matter Physics* (Cambridge Univ. Press, Cambridge UK, 2013).

[84] S. Friedland and J. Milnor, "Dynamical properties of plane polynomial automorphisms", Ergodic Theory Dynam. Systems **9**, 67–99 (1989).

[85] P. M. Gade and R. E. Amritkar, "Spatially periodic orbits in coupled-map lattices", Phys. Rev. E **47**, 143–154 (1993).

[86] R. Giles and C. B. Thorn, "Lattice approach to string theory", Phys. Rev. D **16**, 366–386 (1977).

[87] J. I. Glaser, "Numerical solution of waveguide scattering problems by finite-difference Green's functions", IEEE Trans. Microwave Theory Tech. **18**, 436–443 (1970).

[88] C. Godsil and G. F. Royle, *Algebraic Graph Theory* (Springer, New York, 2013).

[89] G. H. Golub and C. F. Van Loan, *Matrix Computations*, 4th ed. (J. Hopkins Univ. Press, Baltimore, MD, 2013).

[90] G. Grimmett, *Probability on Graphs: : Random Processes on Graphs and Lattices* (Cambridge Univ. Press, 2009).

[91] D. Guido, T. Isola, and M. L. Lapidus, "A trace on fractal graphs and the Ihara zeta function", Trans. Amer. Math. Soc. **361**, 3041–3041 (2009).

[92] B. Gutkin, L. Han, R. Jafari, A. K. Saremi, and P. Cvitanović, "Linear encoding of the spatiotemporal cat map", Nonlinearity **34**, 2800–2836 (2021).

[93] B. Gutkin and V. Osipov, "Classical foundations of many-particle quantum chaos", Nonlinearity **29**, 325–356 (2016).

[94] A. J. Guttmann, "Lattice Green's functions in all dimensions", J. Phys. A **43**, 305205 (2010).

[95] K. T. Hansen, "Alternative method to find orbits in chaotic systems", Phys. Rev. E **52**, 2388–2391 (1995).

[96] P. G. Harper, "Single band motion of conduction electrons in a uniform magnetic field", Proc. Phys. Soc. London, Sect. A **68**, 874–878 (1955).

[97] K. Hashimoto, "Zeta functions of finite graphs and representations of p-adic groups", Adv. Stud. Pure Math. **15**, 211–280 (1989).

[98] J. F. Heagy, "A physical interpretation of the Hénon map", Physica D **57**, 436–446 (1992).

[99] M. Hénon, "A two-dimensional mapping with a strange attractor", Commun. Math. Phys. **50**, 94–102 (1976).

[100] D. L. Hitzl and F. Zele, "An exploration of the Hénon quadratic map", Physica D **14**, 305–326 (1985).

[101] H. Hobrecht and F. Hucht, "Anisotropic scaling of the two-dimensional Ising model I: the torus", SciPost Phys. **7**, 026 (2019).

[102] H. Hobrecht and F. Hucht, "Anisotropic scaling of the two-dimensional Ising model II: surfaces and boundary fields", SciPost Phys. **8**, 032 (2020).

[103] F. Hofbauer and G. Keller, "Zeta-functions and transfer-operators for piecewise linear transformations", J. Reine Angew. Math. (Crelle) **1984**, 100–113 (1984).

[104] D. R. Hofstadter, "Energy levels and wave functions of Bloch electrons in rational and irrational magnetic fields", Phys. Rev. B **14**, 2239–2249 (1976).

[105] T. Horiguchi, "Lattice Green's function for the simple cubic lattice", J. Phys. Soc. Jpn. **30**, 1261–1272 (1971).

[106] T. Horiguchi and T. Morita, "Note on the lattice Green's function for the simple cubic lattice", J. Phys. C **8**, L232 (1975).

[107] M. D. Horton, "Ihara zeta functions of digraphs", Linear Algebra Appl. **425**, 130–142 (2007).

[108] G. Y. Hu and R. F. O'Connell, "Analytical inversion of symmetric tridiagonal matrices", J. Phys. A **29**, 1511 (1996).

[109] G. Y. Hu, J. Y. Ryu, and R. F. O'Connell, "Analytical solution of the generalized discrete Poisson equation", J. Phys. A **31**, 9279 (1998).

[110] A. Hucht, "The square lattice Ising model on the rectangle I: finite systems", J. Phys. A **50**, 065201 (2017).

[111] B. D. Hughes, *Random Walks and Random Environments: Vol. I, Random Walks* (Clarendon Press, Oxford, 1995).

[112] C. A. Hurst and H. S. Green, "New solution of the Ising problem for a rectangular lattice", J. Chem. Phys. **33**, 1059–1062 (1960).

[113] Y. Ihara, "On discrete subgroups of the two by two projective linear group over p-adic fields", J. Math. Soc. Japan **18**, 219–235 (1966).

[114] E. V. Ivashkevich, N. S. Izmailian, and C.-K. Hu, "Kronecker's double series and exact asymptotic expansions for free models of statistical mechanics on torus", J. Phys. A **35**, 5543–5561 (2002).

[115] N. S. Izmailian, "Finite-size effects for anisotropic 2D Ising model with various boundary conditions", J. Phys. A **45**, 494009 (2012).

[116] N. S. Izmailian and C.-K. Hu, "Finite-size effects for the Ising model on helical tori", Phys. Rev. E **76**, 041118 (2007).

[117] N. S. Izmailian, K. B. Oganesyan, and C.-K. Hu, "Exact finite-size corrections for the square-lattice Ising model with Brascamp-Kunz boundary conditions", Phys. Rev. E **65**, 056132 (2002).

[118] K. Jansen, "Lattice field theory", Int. J. Mod. Phys. E **16**, 2638–2679 (2007).

[119] J. Jorgenson and S. Lang, "The ubiquitous heat kernel", in *Mathematics Unlimited - 2001 and Beyond* (Springer, Berlin, 2001), pp. 655–683.

[120] L. P. Kadanoff, *Statistical Physics: Statics, Dynamics and Renormalization* (World Scientific, Singapore, 2000).

[121] G. Kane, *Modern Elementary Particle Physics* (Addison-Wesley, Redwood City, 1987).

[122] A. Karlsson and M. Neuhauser, "Heat kernels, theta identities, and zeta functions on cyclic groups", Contemp. Math. **394**, 177–190 (2006).

[123] S. Katsura and S. Inawashiro, "Lattice Green's functions for the rectangular and the square lattices at arbitrary points", J. Math. Phys. **12**, 1622–1630 (1971).

[124] S. Katsura, S. Inawashiro, and Y. Abe, "Lattice Green's function for the simple cubic lattice in terms of a Mellin-Barnes type integral", J. Math. Phys. **12**, 895–899 (1971).

[125] S. Katsura, T. Morita, S. Inawashiro, T. Horiguchi, and Y. Abe, "Lattice Green's function. Introduction", J. Math. Phys. **12**, 892–895 (1971).

[126] B. Kaufman, "Crystal statistics. II. Partition function evaluated by spinor analysis", Phys. Rev. **76**, 1232–1243 (1949).

[127] V. Khoromskaia and B. N. Khoromskij, "Block circulant and Toeplitz structures in the linearized Hartree-Fock equation on finite lattices: Tensor approach", Comput. Methods Appl. Math. **17**, 43–455 (2017).

[128] Y.-O. Kim, J. Lee, and K. K. Park, "A zeta function for flip systems", Pacific J. Math. **209**, 289–301 (2003).

[129] G. Kirchhoff, "Üeber die Auflösung der Gleichungen, auf welche man bei der Untersuchung der linearen Vertheilung galvanischer Ströme geführt wird", Ann. Phys. Chem. **148**, 497–508 (1847).

[130] O. Knill and F. Tangerman, "Self-similarity and growth in Birkhoff sums for the golden rotation", Nonlinearity **24**, 3115–3127 (2011).

[131] M. Kotani and T. Sunada, "Zeta functions of finite graphs", J. Math. Sci. Univ. Tokyo **7**, 7–25 (2000).

[132] S. Lang, *Linear Algebra* (Addison-Wesley, Reading, MA, 1987).

[133] C. H. Lee, S. Imhof, C. Berger, F. Bayer, J. Brehm, L. W. Molenkamp, T. Kiessling, and R. Thomale, "Topolectrical circuits", Commun. Phys. **1**, 39 (2018).

[134] D. Lenz, F. Pogorzelski, and M. Schmidt, "The Ihara zeta function for infinite graphs", Trans. Amer. Math. Soc. **371**, 5687–5729 (2018).

[135] S. Levit and U. Smilansky, "A new approach to Gaussian path integrals and the evaluation of the semiclassical propagator", Ann. Phys. **103**, 198–207 (1977).

[136] S. Levit and U. Smilansky, "A theorem on infinite products of eigenvalues of Sturm-Liouville type operators", Proc. Amer. Math. Soc. **65**, 299–299 (1977).

[137] H. Liang and P. Cvitanović, "A chaotic lattice field theory in one dimension", J. Phys. A **55**, 304002 (2022).

[138] T. M. Liaw, M. C. Huang, Y. L. Chou, S. C. Lin, and F. Y. Li, "Partition functions and finite-size scalings of Ising model on helical tori", Phys. Rev. E **73**, 041118 (2006).

[139] W. J. Lick, *Difference Equations from Differential Equations* (Springer, Berlin, 1989).

[140] J. S. Lim, *Two-dimensional Signal and Image Processing* (Prentice Hall, Englewood Cliffs, N.J, 1990).

[141] D. Lind and K. Schmidt, "Symbolic and algebraic dynamical systems", in *Handbook of Dynamical Systems*, Vol. 1, edited by B. Hasselblatt and A. Katok (Elsevier, New York, 2002), pp. 765–812.

[142] D. A. Lind, "A zeta function for Z^d-actions", in *Ergodic Theory of Z^d Actions*, edited by M. Pollicott and K. Schmidt (Cambridge Univ. Press, 1996), pp. 433–450.

[143] D. A. Lind and B. Marcus, *An Introduction to Symbolic Dynamics and Coding* (Cambridge Univ. Press, Cambridge, 1995).

[144] R. de la Llave, Variational methods for quasiperiodic solutions of partial differential equations, in Hamiltonian Systems and Celestial Mechanics (HAMSYS–98), edited by J. Delgado, E. A. Lacomba, E. Pérez-Chavela, and J. Llibre (2000).

[145] M. Lüscher and P. Weisz, "Scaling laws and triviality bounds in the lattice ϕ^4 theory (I). One-component model in the symmetric phase", Nucl. Phys. B **290**, 25–60 (1987).

[146] I. Lyberg, "Free energy of the anisotropic Ising lattice with Brascamp-Kunz boundary conditions", Phys. Rev. E **87**, 062141 (2013).

[147] R. S. MacKay, *Renormalisation in Area-preserving Maps* (World Scientific, Singapore, 1993).

[148] R. S. MacKay and J. D. Meiss, "Linear stability of periodic orbits in Lagrangian systems", Phys. Lett. A **98**, 92–94 (1983).

[149] J. Mallet-Paret and S.-N. Chow, "Pattern formation and spatial chaos in lattice dynamical systems. I", IEEE Trans. Circuits Systems I Fund. Theory Appl. **42**, 746–751 (1995).

[150] J. Mallet-Paret and S.-N. Chow, "Pattern formation and spatial chaos in lattice dynamical systems. II", IEEE Trans. Circuits Systems I Fund. Theory Appl. **42**, 752–756 (1995).

[151] E. C. Marino, *Quantum Field Theory Approach to Condensed Matter Physics* (Cambridge Univ. Press, Cambridge UK, 2017).

[152] P. A. Martin, "Discrete scattering theory: Green's function for a square lattice", Wave Motion **43**, 619–629 (2006).

[153] B. M. McCoy and T. T. Wu, *The Two-Dimensional Ising Model*, 2nd ed. (Dover, 1973).

[154] B. D. Mestel and I. Percival, "Newton method for highly unstable orbits", Physica D **24**, 172 (1987).

[155] H. B. Meyer, "Lattice QCD: A brief introduction", in *Lattice QCD for Nuclear Physics*, edited by H.-W. Lin and H. B. Meyer (Springer, York New, 2015), pp. 1–34.

[156] D. Micciancio and S. Goldwasser, *Complexity of Lattice Problems - A Cryptographic Perspective* (Springer, New York, 2002).

[157] M. Michałek and B. Sturmfels, *Invitation to Nonlinear Algebra* (MPI Leipzig, 2020).

[158] N. Miguel, C. Simó, and A. Vieiro, "From the Hénon conservative map to the Chirikov standard map for large parameter values", Regul. Chaotic Dyn. **18**, 469–489 (2013).

[159] R. Miles, "A dynamical zeta function for group actions", Monatsh. Math. **182**, 683–708 (2016).

[160] I. Montvay and G. Münster, *Quantum Fields on a Lattice* (Cambridge Univ. Press, Cambridge, 1994).

[161] T. Morita, "Useful procedure for computing the lattice Green's function - square, tetragonal, and bcc lattices", J. Math. Phys. **12**, 1744–1747 (1971).

[162] T. Morita and T. Horiguchi, "Calculation of the lattice Green's function for the bcc, fcc, and rectangular lattices", J. Math. Phys. **12**, 986–992 (1971).

[163] G. Münster, "Lattice quantum field theory", Scholarpedia **5**, 8613 (2010).

[164] G. Münster and M. Walzl, Lattice gauge theory - A short primer, 2000.

[165] J. Nielsen, "Über die Minimalzahl der Fixpunkte bei den Abbildungstypen der Ringflächen", Math. Ann. **82**, 83–93 (1920).

[166] J. Ningyuan, C. Owens, A. Sommer, D. Schuster, and J. Simon, "Time- and site-resolved dynamics in a topological circuit", Phys. Rev. X **5**, 021031 (2015).

[167] Y. Okabe, K. Kaneda, M. Kikuchi, and C.-K. Hu, "Universal finite-size scaling functions for critical systems with tilted boundary conditions", Phys. Rev. E **59**, 1585–1588 (1999).

[168] L. Onsager, "Crystal statistics. I. A Two-dimensional model with an order-disorder transition", Phys. Rev. **65**, 117–149 (1944).

[169] G. Papathanasiou and C. B. Thorn, "Worldsheet propagator on the lightcone worldsheet lattice", Phys. Rev. D **87**, 066005 (2013).

[170] W. Parry, "On the β-expansions of real numbers", Acta Math. Acad. Sci. Hung. **11**, 401–416 (1960).

[171] R. Peierls, "Zur Theorie des Diamagnetismus von Leitungselektronen", Z. Phys. **80**, 763–791 (1933).

[172] I. Percival and F. Vivaldi, "A linear code for the sawtooth and cat maps", Physica D **27**, 373–386 (1987).

[173] A. Poghosyan, N. Izmailian, and R. Kenna, "Exact solution of the critical Ising model with special toroidal boundary conditions", Phys. Rev. E **96**, 062127 (2017).

[174] A. Politi and A. Torcini, "Periodic orbits in coupled Hénon maps: Lyapunov and multifractal analysis", Chaos **2**, 293–300 (1992).

[175] A. Politi, A. Torcini, and S. Lepri, "Lyapunov exponents from node-counting arguments", J. Phys. IV **8**, 263 (1998).

[176] M. Pollicott, Dynamical zeta functions, in Smooth Ergodic Theory and Its Applications, Vol. 69, edited by A. Katok, R. de la Llave, Y. Pesin, and H. Weiss (2001), pp. 409–428.

[177] C. Pozrikidis, *An Introduction to Grids, Graphs, and Networks* (Oxford Univ. Press, Oxford , UK, 2014).

[178] L. Qi, H. Chen, and Y. Chen, *Tensor Eigenvalues and Their Applications* (Springer, Singapore, 2018).

[179] P. Ramond, *Field Theory* (Routledge, 1981).

[180] P. Ren, T. Aleksić, D. Emms, R. C. Wilson, and E. R. Hancock, "Quantum walks, Ihara zeta functions and cospectrality in regular graphs", Quantum Inf. Process. **10**, 405–417 (2010).

[181] A. Rényi, "Representations for real numbers and their ergodic properties", Acta Math. Acad. Sci. Hung. **8**, 477–493 (1957).

[182] M. Rezghi and L. Eldén, "Diagonalization of tensors with circulant structure", Linear Algebra Appl. **435**, 422–447 (2011).

[183] K. Richter, J. D. Urbina, and S. Tomsovic, "Semiclassical roots of universality in many-body quantum chaos", J. Phys. A **55**, 453001 (2022).

[184] O. E. Rössler, "An equation for continuous chaos", Phys. Lett. A **57**, 397–398 (1976).

[185] H. J. Rothe, *Lattice Gauge Theories - An Introduction* (World Scientific, Singapore, 2005).

[186] I. Sato, "Bartholdi zeta functions of group coverings of digraphs", Far East J. Math. Sci. **18**, 321–339 (2005).

[187] J.-P. Serre, *Trees* (Springer, Berlin, 1980).

[188] R. Shankar, *Quantum Field Theory and Condensed Matter* (Cambridge Univ. Press, Cambridge UK, 2017).

[189] C. L. Siegel and K. Chandrasekharan, *Lectures on the Geometry of Numbers* (Springer Berlin Heidelberg, Berlin, Heidelberg, 1989).

[190] C. Simó, "On the Hénon-Pomeau attractor", J. Stat. Phys. **21**, 465–494 (1979).

[191] B. Simon, "Almost periodic Schrödinger operators: A review", Adv. Appl. Math. **3**, 463–490 (1982).

[192] J. Smit, *Introduction to Quantum Fields on a Lattice* (Cambridge Univ. Press, Cambridge, 2002).

[193] R. Sommer, Introduction to Lattice Gauge Theories, tech. rep. (Humboldt Univ., 2015).

[194] H. M. Stark and A. A. Terras, "Zeta functions of finite graphs and coverings", Adv. Math. **121**, 124–165 (1996).

[195] J. Stephenson and D. T. Ridgway, "Formulae for cycles in the Mandelbrot set II", Physica A **190**, 104–116 (1992).

[196] D. Sterling and J. D. Meiss, "Computing periodic orbits using the anti-integrable limit", Phys. Lett. A **241**, 46–52 (1998).

[197] D. G. Sterling, Anti-integrable Continuation and the Destruction of Chaos, PhD thesis (Univ. Colorado, Boulder, CO, 1999).

[198] D. G. Sterling, H. R. Dullin, and J. D. Meiss, "Homoclinic bifurcations for the Hénon map", Physica D **134**, 153–184 (1999).

[199] I. Stewart and D. Gökaydin, "Symmetries of quotient networks for doubly periodic patterns on the square lattice", Int. J. Bifur. Chaos **29**, 1930026 (2019).

[200] R. Suarez, "Difference equations and a principle of double induction", Math. Mag. **62**, 334–339 (1989).

[201] T. Sunada, *Topological Crystallography* (Springer, Tokyo, 2013).

[202] A. Tarfulea and R. Perlis, "An Ihara formula for partially directed graphs", Linear Algebra Appl. **431**, 73–85 (2009).

[203] A. Terras, *Zeta Functions of Graphs: A Stroll through the Garden* (Cambridge Univ. Press, 2010).

[204] M. Toda, *Theory of Nonlinear Lattices* (Springer, Berlin, 1989).

[205] J. H. Van Vleck, "The correspondence principle in the statistical interpretation of quantum mechanics", Proc. Natl. Acad. Sci. **14**, 178–188 (1928).

[206] G. Venezian, "On the resistance between two points on a grid", Am. J. Phys **62**, 1000–1004 (1994).

[207] Y. Colin de Verdière, "Spectrum of the Laplace operator and periodic geodesics: thirty years after", Ann. Inst. Fourier **57**, 2429–2463 (2007).

[208] D. Viswanath, "The Lindstedt-Poincaré technique as an algorithm for finding periodic orbits", SIAM Rev. **43**, 478–496 (2001).

[209] D. Viswanath, "Symbolic dynamics and periodic orbits of the Lorenz attractor", Nonlinearity **16**, 1035–1056 (2003).

[210] D. Viswanath, "The fractal property of the Lorenz attractor", Physica D **190**, 115–128 (2004).

[211] U.-J. Wiese, An Introduction to Lattice Field Theory, tech. rep. (Univ. Bern, 2009).

[212] I. Wigman, "Counting singular matrices with primitive row vectors", Monatsh. Math. **144**, 71–84 (2005).

[213] Wikipedia contributors, Index of a subgroup — Wikipedia, The Free Encyclopedia, 2022.

[214] H. S. Wilf, *Generatingfunctionology* (Academic Press, New York, 1994).

[215] S. V. Williams, X. Wang, H. Liang, and P. Cvitanović, Nonlinear chaotic lattice field theory, In preparation, 2023.

[216] U. Wolff, "Triviality of four dimensional ϕ^4 theory on the lattice", Scholarpedia **9**, 7367 (2014).

[217] W. L. Wood, "Periodicity effects on the iterative solution of elliptic difference equations", SIAM J. Numer. Anal. **8**, 439–464 (1971).

[218] J. Woods, *Multidimensional Signal, Image, and Video Processing and Coding* (Academic Press, Amsterdam, 2012).

[219] F. Y. Wu, "Theory of resistor networks: the two-point resistance", J. Phys. A **37**, 6653–6673 (2004).

[220] M.-C. Wu and C.-K. Hu, "Exact partition functions of the Ising model on M x N planar lattices with periodic-aperiodic boundary conditions", J. Phys. A **35**, 5189–5206 (2002).

[221] Z.-J. Xie, X.-Q. Jin, and Y.-M. Wei, "A fast algorithm for solving circulant tensor systems", Lin. Multilin. Algebra **65**, 1894–1904 (2016).

[222] Y. Yamasaki, "An explicit prime geodesic theorem for discrete tori and the hypergeometric functions", Math. Z. **289**, 361–376 (2017).

[223] Q. Zhilin, A. Gangal, M. Benkun, and T. Gang, "Spatiotemporally periodic patterns in symmetrically coupled map lattices", Phys. Rev. E **50**, 163–170 (1994).

[224] D. Zhou, Y. Xiao, and Y.-H. He, "Seiberg duality, quiver gauge theories, and Ihara's zeta function", Int. J. Mod. Phys. A **30**, 1550118 (2015).

[225] R. M. Ziff, C. D. Lorenz, and P. Kleban, "Shape-dependent universality in percolation", Physica A **266**, 17–26 (1999).

Appendix D. Reversal' LC21blog

The latest entry at the bottom of this section, page 66

Internal discussions of [137] arXiv:2201.11325 (uploaded 27 Jan 2022) edits: we had saved text not used in [137] here, for possible reuse in [55], or elsewhere.

Tentative title: "Is there anything cats cannot do?"

2016-11-18 Predrag A theory of turbulence that has done away with *dynamics*? We rest our case.
The deep insight here is the realization that the *Hill determinant*, i.e., the volume of the *orbit Jacobian matrix* (figure **??** and **??**) partitions system's state space.

2016-11-18 Predrag The dynamics is breathtakingly simple on the reciprocal lattice. Spatial period-n primitive cell maps onto a regular n-gon in the reciprocal lattice. Time reversal fixes the symmetric solutions to sit on the symmetry axes, the boundaries of the fundamental domain. Lattice shift r_j maps out the G-orbit by running on circles, and orbits visit the $1/2n$ wedge only once, so the points in the fundamental domain represent an orbit each.
with all reciprocal lattice Brillioun zone solutions orbits in an $1/n$ sliver of a n-gon. No self-respecting crystallographer would be drawing longer and longer periodic states (**??**)-(**??**) - they eventually run off the sheet of paper, no matter how wide. A professional crystallographer plots all periodic states snugly together in the first Brillouin zone, where the translational orbit of a periodic state is -literally- a circle, symmetric periodic states sit on boundaries of point group's fundamental domain, and everything is maximally diagonalized in term's of space group G irreps.
Consider

$$\rho_{\vec{G}}(\vec{x}) = e^{i\vec{G}\cdot\vec{r}(\vec{x})}\,,$$

where $\vec{G}$ is a reciprocal lattice vector. By definition, $\vec{G}\cdot\vec{a}$ is an integer multiple of 2π, $\rho_{\vec{G}}=1$ for lattice vectors. For any other state, reciprocal periodic state is given by

$$e^{i\vec{G}\cdot\vec{u}(\vec{x})} \neq 1\,.$$

When a cube is a building block that tiles a $3D$ cubic lattice, it is referred to as the 'elementary' or 'Wigner-Seitz' cell, and its Fourier transform is called 'the first Brillouin zone' in 'the reciprocal space'.
the time-reversal pairs to be the complex-conjugate pairs in Fourier space, as C_∞ shift moves them in opposite directions.
The eigenvectors of the translation operator which satisfy the periodicity of the Bravais lattice are plane waves of form:

$$f_{\mathbf{k}}(\mathbf{z}) = e^{i\mathbf{k}\cdot\mathbf{z}}\,, \quad \mathbf{k}\in\overline{\mathcal{L}}\,, \tag{D.1}$$

where the wave vector $\mathbf{k}$ is on the reciprocal lattice $\overline{\mathcal{L}}$.
A general plane wave does not satisfy the periodicity, unless

$$e^{ik\cdot R} = 1\,. \tag{D.2}$$

Since R is a vector from the Bravais lattice $\mathcal{L}$, the wave vector $\mathbf{k}$ must lie in the reciprocal lattice of $\mathcal{L}$:

$$\mathbf{k} \in \mathcal{L}^*\,, \quad \mathcal{L}^* = \{m\mathbf{b}\,|\,m \in \mathbb{Z}\}\;, \tag{D.3}$$

where the primitive reciprocal lattice vectors $\mathbf{b}$ satisfies:

$$\mathbf{b}\cdot\mathbf{a} = 2\pi\,. \tag{D.4}$$

Barvinok arXiv:/math/0504444:
Let V be a d-dimensional real vector space with the scalar product $\langle\cdot,\cdot\rangle$ and the corresponding Euclidean norm $\|\cdot\|$. Let $\mathcal{L} \subset V$ be a lattice and let $\mathcal{L}^* \subset V$ be the *dual* or the *reciprocal* lattice

$$\mathcal{L}^* = \Big\{x \in V : \quad \langle x, y\rangle \in \mathbb{Z} \quad \text{for all} \quad y \in \mathcal{L}\Big\}\,.$$

2021-08-10 Han When we write period-n periodic states as n-dimensional vectors, and write the shift operator r as a $[n \times n]$ matrix (**??**) which applies cyclic permutation to the periodic state, the matrix representation of shift operators forms a permutation representation of the cyclic translation group C_n. This permutation representation is a reducible representation, i.e., it can be block diagonalized by a similarity transformation. Each block on the diagonal is an irreducible representation (irrep).
The abelian group C_n only has 1-dimensional irreps. The permutation representation of C_n can be diagonalized by discrete Fourier transform. After the transform the representation of the shift operator becomes,

$$r^m = \begin{pmatrix} 1 & & & & \\ & \omega^m & & & \\ & & \omega^{2m} & & \\ & & & \ddots & \\ & & & & \omega^{(n-1)m} \end{pmatrix}\,, \quad \omega = \mathrm{e}^{2\pi\mathrm{i}/n}\,, \tag{D.5}$$

with periodic states projected onto 1-dimensional subspaces in which action of the shift operators is given by corresponding irrep. As we transform the permutation representation of the shift operator into the block diagonal form, the periodic states $(\phi_0, \phi_1, \phi_2, \ldots, \phi_{n-1})$ are spanned by the Fourier modes basis, with components $(\tilde\phi_0, \tilde\phi_1, \tilde\phi_2, \ldots, \tilde\phi_{n-1})$. When the shift operator acts on the periodic state: $\Phi \to r\Phi$, the irreducible representations act on the components in the corresponding subspace: $\tilde\phi_k \to \omega^k\tilde\phi_k$.
Dihedral group
In the n-dimensional space of the period-n periodic states, the permutation representation of the Dihedral group D_n can be generated by the shift operator

matrix representation (**??**) and the reflection operator matrix representation:

$$\sigma = \begin{pmatrix} 1 & & & & 0 \\ & & & 0 & 1 \\ & & \cdot^{\cdot^{\cdot}} & 1 & \\ & 0 & \cdot^{\cdot^{\cdot}} & & \\ 0 & 1 & & & \end{pmatrix} . \tag{D.6}$$

The Dihedral group D_n has: 2 1-dimensional irreps and $[(n-1)/2]$ 2-dimensional irreps if n is odd, or 4 1-dimensional irreps and $(n/2-1)$ 2-dimensional irreps if n is even. If n is odd, the permutation representation can be block diagonalized into irreps: $A_0 \oplus E_1 \oplus \ldots \oplus E_{(n-1)/2}$. If n is even, the permutation representation can be block diagonalized into irreps: $A_0 \oplus B_1 \oplus E_1 \oplus \ldots \oplus E_{n/2-1}$.

2021-09-02 Predrag Why do you mark 1/8 in figures **??** and **??**, when the units are 1/7's? I see. You have $1/\sqrt{3}$ and π's floating around, unless you redefine units...

2021-07-07 Predrag Experimenting with (D.7) by:
a flip across the kth axis, $k = 0, 1, 2, \cdots, n-1$,

$$\text{dihedral } D_n : \quad H_{n,k} = \langle r, \sigma_k = r^k\sigma \mid \sigma_k r \sigma_k = r^{-1}\,,\; r^n = \sigma_k^2 = 1 \rangle , \tag{D.7}$$

that Han had replaced with (**??**) and n with $|n|$ in (**??**).

2021-07-07 Predrag A presentation of the *infinite dihedral group* [128] is

$$D_\infty = \left\langle r_i, \sigma_j \mid r_i\sigma_j = \sigma_j r_{-i};\; \sigma_j^2 = 1;\; i, j \in \mathbb{Z} \right\rangle . \tag{D.8}$$

2021-08-10 Predrag dropped:
Applying the projection operator $P_{0-} = \frac{1}{2}(\mathbf{1} - \sigma_0)/2$ we obtain a periodic state

$$\cdots \underline{y_4}\,\underline{y_3}\,\underline{y_2}\,\underline{y_1}\boxed{0}y_1 y_2 y_3 y_4 \cdots , \tag{D.9}$$

antisymmetric under reflection, where the field $\boxed{0} = (\phi_0 - \phi_0)/2 = 0$ at the reflection lattice site 0 vanishes by antisymmetry, while the rest, $y_j = (\phi_j - \phi_{-j})/2$, are pairwise antisymmetric under the reflection σ. The underline indicates the negative of, i.e., $\underline{y_j} = -y_j$.
Applying the antisymmetric projection operator $P_{1-} = \frac{1}{2}(\mathbf{1} - \sigma r)/2$ we obtain a periodic state

$$\cdots \underline{y_4}\,\underline{y_3}\,\underline{y_2}\,\underline{y_1}\,| y_1 y_2 y_3 y_4 \cdots , \tag{D.10}$$

antisymmetric under reflection, where $y_j = (\phi_j - \phi_{1-j})/2$, are pairwise antisymmetric under the reflection σ_1.

2021-10-29 Predrag Dropped: Cat maps are beloved by ergodicists and statistical mechanicians because, even though the field (q_t, p_t) is 2-dimensional, for integer values of the stretching parameter s, a cat map has a finite alphabet linear code, just like the Bernoulli map, and its unit torus can be tiled by two rectangles,

[2020-12-17 Predrag] Link to the ChaosBook.

in analogy with the forward-in-time Bernoulli map subinterval partitioning of figure **??**.

2021-10-29 Predrag Dropped: The Lagrangian formulation requires only temporal periodic states and their actions, replacing the phase space 'cat map' (**??**) by a 'temporal cat' lattice (**??**). The temporal cat has no generating partition analogue of the Adler-Weiss partition for a Hamiltonian cat map (see

[2020-12-17 Predrag] Link to the ChaosBook.

). As we have shown here, no funky Hamiltonian state space partitioning magic (such as

[2020-12-17 Predrag] Link to the ChaosBook.

) is needed to count the periodic states of a temporal cat. Not only are no such partitions needed to solve the system, but the Lagrangian,

2021-08-12 Predrag Sidney will chuckle at this comment: The usual $a\phi_t^2$ form (**??**) might be preferable, as the 'a' is a stretching parameter, just like in (**??**). See section **??** Temporal Hénon.

2021-08-17 Predrag See (**??**). We also MUST explain the relation to literature, as in the post including (**??**).

2020-12-17 Predrag Link to the ChaosBook? or drop?
In section **??** we review the traditional cat map in its Hamiltonian formulation. (but relegate to the explicit Adler-Weiss generating partition of the cat map state space).
We evaluate and cross-check Hill determinants by two methods, either the 'fundamental fact' evaluation, or by the discrete Fourier transform diagonalization, section **??**.

2021-10-13 Predrag Is there a - sign specific to Sidney's definition of the Hénon orbit Jacobian matrix Han and Predrag have to redefine both temporal cat and temporal Hénon orbit Jacobian matrix throughout, so we do not pick up an extraneous '-' sign for odd period periodic states. See also (**??**), and Pozrikidis [177] (click here) eq. (1.8.2). The main thing is to have a Laplacian with positive eigenvalues, right? Maybe not, the main thing is to have hyperbolic eigenvalues for $s > 2$. Rethink. determinants in periodic orbit formulas.
$Z[\mathsf{J}]$ notation extracted from *lattFTnotat.tex*, called *by lattFT.tex*.
, in field theorist's parlance, m_z are 'sources', and
The orbit Jacobian matrix $\mathcal{J}[\Phi]$ is best understood by starting with the period-n primitive cell stability.
As in section **??**, the fundamental parallelepiped given the stretching of the n-dimensional state space unit hypercube $\Phi \in [0,1)^n$ by the orbit Jacobian matrix counts periodic states, with the admissible periodic states of period T constrained to field values within $0 \leq \phi_t < 1$. The fundamental parallelepiped contains images of all periodic states Φ_{M}, which are then translated by integer winding numbers M into the origin, in order to satisfy the fixed point condition (**??**).

2021-10-21 Predrag Han, RECHECK all m_t, as well as formulas starting with (**??**)!!! Bernoulli m_t in (**??**) conflicted with the old definition (**??**), so I changed (**??**).

When the force is proportional to displacement, that is, when Hooke's law is obeyed, the spring is said to be linear, the potential is quadratic.

A matrix $\mathbb{J}$ with no eigenvalue on the unit circle is called hyperbolic.

Ignoring (mod 1) for a moment, we can use (**??**) to eliminate p_t from (**??**) and rewrite the kicked rotor equation as the

For the problem at hand, it pays to go from the Hamiltonian (configuration, momentum) phase space formulation to the discrete Lagrangian (ϕ_{t-1}, ϕ_t) formulation.

temporal lattice condition

'Temporal' again refers to the discretized time $1d$ lattice

In atomic physics applications, the values of the angle q differing by integers are identified, but the momentum p is unbounded. In dynamical systems theory one compactifies the momentum as well, by adding (mod 1) to (**??**), as for the Bernoulli map (**??**). This reduces the phase space to a square $[0,1) \times [0,1)$ of unit area, with the opposite edges identified, i.e., 2-torus.

Thom-Anosov diffeomorphism

Cat maps with the same s are equivalent up to a similarity transformation, so it suffices to work out a single convenient realization, as we shall do here for the Percival-Vivaldi [172] 'two-configuration representation' (**??**).

2021-11-29 Predrag !!!WARNING!!! Following Han (**??**), we are changing the sign of the action $S[\Phi]$ and the orbit Jacobian matrix, as in (**??**), THROUGHOUT! (Totally Predrag's fault). This makes spatiotemporal cat and ϕ^4 theory action strictly positive for $s > 2$, as needed for the probability interpretation (**??**). Han, Sidney and Predrag have to redefine temporal cat, spatiotemporal cat and temporal Hénon orbit Jacobian matrices throughout, to avoid the extraneous '-' sign for odd period periodic states. See also (**??**), and Pozrikidis [177] (click here) eq. (1.8.2).

2016-11-08 Predrag Say: THE BIG DEAL is

for d-dimensional field theory, symbolic dynamics is not one temporal sequence with a huge alphabet, but d-dimensional spatiotemporal tiling by a finite alphabet

2021-12-27 Predrag removed:

Hill determinant: time-evolution evaluation

However, in classical and statistical mechanics, one often computes the Hill determinant using a Hamiltonian, or 'transfer matrix' formulation.

Define

$$\hat{\phi}_t = \begin{bmatrix} \phi_{t-1} \\ \phi_t \end{bmatrix}, \quad \hat{\mathsf{m}}_t = \begin{bmatrix} 0 \\ m_t \end{bmatrix},$$

where the hat $\hat{}$ indicates a 2-dimensional 'two-configuration' [172] lattice site t state.

The 1-dimensional field theory three-term recurrence (**??**) written in the Percival-Vivaldi [172] 'two-configuration representation' (**??**).

$\mathcal{J}_1$ is the spatial $[L \times L]$ orbit Jacobian matrix of $d = 1$ temporal cat form (**??**), This proves that $\det \hat{\mathcal{J}}$ of the 'Hamiltonian' or 'two-configuration' $[2Ln \times 2Ln]$ 'phase space' orbit Jacobian matrix $\hat{\mathcal{J}}$ defined by (**??**) equals the 'Lagrangian' Hill determinant of the $[Ln \times Ln]$ orbit Jacobian matrix $\mathcal{J}$.

2021-12-26 Han I think (**??**–**??**) should be written as:

$$q_{t+1} = q_t + p_{t+1} \qquad (\mathrm{mod}\ 1), \tag{D.11}$$

$$p_{t+1} = p_t + P(q_t)\,. \tag{D.12}$$

Otherwise the angle of the rotor q is not constrained to $[0, 1)$.
Predrag: you are right, corrected.

2021-12-29 Predrag The state space $\mathcal{M}$ of a D_∞ invariant dynamical is union of 4 subspaces of periodic states 4 distinct symmetries (see figure **??**)

$$\mathcal{M} = \mathcal{M}_a \cup \mathcal{M}_o \cup \mathcal{M}_{ee} \cup \mathcal{M}_{ee}\,, \tag{D.13}$$

where

$\Phi \in \mathcal{M}_a$ *no reflection symmetry* (**??**), see figure **??**
orbit $p = \{\Phi, r\Phi, \cdots, r_{n-1}\Phi, \sigma\Phi, \sigma_1\Phi, \cdots, \sigma_{n-1}\Phi\}$

$\Phi \in \mathcal{M}_o$ *odd period, reflection-symmetric:* (**??**) see figure **??**
orbit $p = \{\Phi, r\Phi, \cdots, r_{n-1}\Phi\}$

$\Phi \in \mathcal{M}_{ee}$ *even period, even reflection-symmetric:* (**??**)

$\Phi \in \mathcal{M}_{eo}$ *even period, odd reflection-symmetric:* (**??**).

Let $\mathcal{M}_a$ be the set of pairs of asymmetric orbits (**??**), each element of the set a forward-in-time orbit and the time-reversed orbit. If prime cycle $p \in \mathcal{M}_a$ exists, it and each of its repeats counts as 1:

$$1/\zeta_p(t) = \exp\Big(-\sum_{r=1}^{\infty} \frac{1}{2n_p r} t^{2n_p r}\Big) = \sqrt{1 - t^{2n_p}}\,. \tag{D.14}$$

prime periodic state $p \in \mathcal{M}_o$ exists, periodic state invariant under the dihedral group $H_{n,k}$, n_p values of k

$$1/\zeta_p(t) = \exp\Big(-\sum_{r=1}^{\infty} \frac{1}{r} t^{n_p r}\Big) = \exp\Big(-\sum_{r=1}^{\infty} \frac{t^{n_p}}{1 - t^{n_p}}\Big)\,. \tag{D.15}$$

prime cycle $p \in \mathcal{M}_{ee}$ exists

$$1/\zeta_p(t) = \exp\Big(-\sum_{m=1}^{\infty} \Big\{ N_{2m-1,0}\, t^{2m-1} + (N_{2m,0} + N_{2m,1})\, \frac{t^{2m}}{2} \Big\}\Big)\,. \tag{D.16}$$

Let $\mathcal{M}_s$ be the collection of finite orbits with time reversal (flip) symmetry, and $\mathcal{M}_a$ be the collection of the pairs of orbits without time reversal symmetry, each an orbit and the flipped orbit. A finite orbit p is a periodic points set

$$p = \{\phi, f(\phi), \ldots, f^{n_p - 1}(\phi)\}$$

if $p \in \mathcal{M}_s$, and

$$p = \{\phi, f(\phi), \ldots, f^{k-1}(\phi)\} \cup \{\sigma(\phi), f \circ \sigma(\phi), \ldots, f^{k-1} \circ \sigma(\phi)\}$$

if $p \in \mathcal{M}_a$, where $k = n_p/2$.
If $p \in \mathcal{M}_s$,

$$\zeta_p(t) = \sqrt{\frac{1}{1-t^{2n_p}}} \exp\left(\frac{t^{n_p}}{1-t^{n_p}}\right) , \tag{D.17}$$

The product form of the zeta function is:

$$1/\zeta_{\mathrm{KLP}}(t) = \prod_{p_1 \in O_1} \sqrt{1-t^{2n_{p_1}}} \; \exp\left(-\frac{t^{n_{p_1}}}{1-t^{n_{p_1}}}\right) \prod_{p_2 \in \mathcal{M}_a} (1-t^{n_{p_2}}) \,. \tag{D.18}$$

==

How to count the number of periodic states for temporal cat?
No symmetry periodic states Hill determinant:

$$N_n = \prod_{j=0}^{n-1} \left(s - 2\cos\frac{2\pi j}{n}\right) .$$

The products of eigenvalues for the C_n discrete Fourier case follows from (**??**):

$$\prod_{j=0}^{n-1} \left(s - 2\cos\frac{2\pi j}{n}\right) = (\Lambda^{n/2} - \Lambda^{-n/2})^2 , \tag{D.19}$$

It's a square, because of the D_n symmetry. Consider even, odd casses, use $\cos 0 = 1$, $\cos\pi = -1$, $\cos(-\theta) = \cos\theta$. The product over non-trivial eigenvalues is:

$$n = 2m M_{n,0} = \prod_{j=1}^{m-1} \left(s - 2\cos\frac{\pi j}{m}\right) = \frac{|\Lambda^{n/2} - \Lambda^{-n/2}|}{\mu\sqrt{\mu^2+4}} , \tag{D.20}$$

$$n = 2m-1 M_{n,1} = \prod_{j=1}^{m-1} \left(s - 2\cos\frac{2j\pi}{2m-1}\right) = \frac{|\Lambda^{n/2} - \Lambda^{-n/2}|}{\mu} , \tag{D.21}$$

Next, look at the *symmetric* periodic states Hill determinants:
For odd $n = 2m-1$,

$$N_{n,1} = \prod_{j=0}^{m-1} \left(s - 2\cos\frac{2\pi j}{n}\right) = \mu M_{n,1} . \tag{D.22}$$

For $n = 2m$,

$$N_{n,1} = \prod_{j=0}^{m-1} \left(s - 2\cos\frac{2\pi j}{n}\right)$$
$$N_{n,0} = (s+2)\, N_{n,1} , \tag{D.23}$$

and

$$\frac{1}{2}\left(N_{n,0} + N_{n,1}\right) = \frac{\mu^2+5}{2} \prod_{j=0}^{m-1} \left(s - 2\cos\frac{2\pi j}{n}\right) = \frac{\mu^2+5}{2\mu} \sqrt{\frac{(\Lambda^n + \Lambda^{-n} - 2)}{\mu^2+4}} \tag{D.24}$$

The number of periodic states can be written as polynomials: For $n = 2m - 1$:

$$N_{n,0} = \mu\left(\Lambda^{n/2} - \Lambda^{-n/2}\right) = \mu^2\Lambda^{-1/2}\left(\Lambda^m - \Lambda^{-m+1}\right) . \tag{D.25}$$

For $n = 2m$:

$$\frac{1}{2}\left(N_{n,0} + N_{n,1}\right) = \frac{s+3}{2(\Lambda - \Lambda^{-1})}\left(\Lambda^{n/2} - \Lambda^{-n/2}\right) = \frac{\mu^2 + 5}{2\mu\sqrt{\mu^2+4}}\left|\Lambda^m - \Lambda^{-m}\right| . \tag{D.26}$$

Now we can compute the $h(t)$ from (D.55)

$$\begin{aligned} h(t) &= \sum_{m=1}^{\infty}\left[N_{2m-1,0}\, t^{2m-1} + \left(N_{2m,0} + N_{2m,1}\right)\frac{t^{2m}}{2}\right] \\ &= \mu\frac{\Lambda^{1/2}t}{1-\Lambda t^2} - \mu\frac{\Lambda^{-1/2}t}{1-\Lambda^{-1}t^2} \\ &\quad + \frac{\mu^2+5}{2(\Lambda-\Lambda^{-1})}\frac{\Lambda t^2}{1-\Lambda t^2} - \frac{\mu^2+5}{2(\Lambda-\Lambda^{-1})}\frac{\Lambda^{-1}t^2}{1-\Lambda^{-1}t^2} . \end{aligned} \tag{D.27}$$

Using (D.54) we have the symmetric periodic states part of the Kim-Lee-Park zeta function. Expanding this zeta function using (D.37), we have:

$$\begin{aligned} -t\frac{\partial}{\partial t}(\ln e^{-h(t)}) &= t + 6t^2 + 12t^3 + 36t^4 + 55t^5 + 144t^6 \\ &\quad + 203t^7 + 504t^8 + 684t^9 + 1650t^{10} + \dots , \end{aligned} \tag{D.28}$$

which is in agreement with (D.37) and table **??**.

Appendix D.1. Counting periodic states

Given the topological zeta function (D.52) we can count the number of periodic states from the generating function:

> [2021-08-25 Predrag] We have the counts of the periodic states N_n, $N_{n,k}$ already, from (D.53), so why don't we reverse the logic, start here, and get the zeta function (D.54) by integration? Mention that this is an example of Lind zeta function [142] (**??**) without ever writing it down, so we do not have to explain it? It's a side issue for us, really.

$$\frac{-t\frac{d}{dt}(1/\zeta_\sigma(t))}{1/\zeta_\sigma(t)} = \sum_{n=1}^{\infty} N_n t^{2n} + \sum_{n=1}^{\infty}\sum_{k=0}^{n-1} N_{n,k}t^n = \sum_{m=1}^{\infty} a_m t^m , \tag{D.29}$$

where the coefficients are:

$$a_m = \begin{cases} \sum_{k=0}^{m-1} N^\sigma_{m,k} = mN^\sigma_{m,0} , & m \text{ is odd} , \\ N_{m/2} + \sum_{k=0}^{m-1} N^\sigma_{m,k} = N_{m/2} + \frac{m}{2}\left(N^\sigma_{m,0} + N^\sigma_{m,1}\right) , & m \text{ is even} . \end{cases} \tag{D.30}$$

Using the product formula of topological zeta function (D.18) and the numbers of orbits with length up to 5 from the table **??**, we can write the topological zeta function:

$$1/\zeta_\sigma(t) = \sqrt{1-t^2}\exp\left(-\frac{t}{1-t}\right)(1-t^4)\exp\left(-\frac{2t^2}{1-t^2}\right)\left(\sqrt{1-t^6}\right)^3$$
$$\exp\left(-\frac{3t^3}{1-t^3}\right)(1-t^6)(1-t^8)^3\exp\left(-\frac{6t^4}{1-t^4}\right)$$
$$(1-t^8)^2(1-t^{10})^5\exp\left(-\frac{10t^5}{1-t^5}\right)(1-t^{10})^6\dots. \tag{D.31}$$

The generating function is:

$$\frac{-t\frac{d}{dt}(1/\zeta_\sigma)}{1/\zeta_\sigma} = t + 7t^2 + 12t^3 + 41t^4 + 55t^5 + \dots, \tag{D.32}$$

which is in agreement with (D.30), where the N_n and N_n^σ are the C_n and SF_n in the table **??**.

We are not able to retrieve the numbers of fixed points by their symmetry groups using this topological zeta function (D.52), unless we rewrite the topological zeta function with two variables:

$$\zeta_\sigma(t,u) = \exp\left(\sum_{n=1}^{\infty}\frac{N_n}{2n}t^{2n} + \sum_{n=1}^{\infty}\sum_{k=0}^{n-1}\frac{N_{n,k}}{n}u^n\right). \tag{D.33}$$

Using this topological zeta function $\zeta_\sigma(t,u)$ we can write two generating functions:

$$\frac{-t\frac{\partial}{\partial t}(1/\zeta_\sigma(t,u))}{1/\zeta_\sigma(t,u)} = \sum_{n=1}^{\infty}N_n t^{2n}, \tag{D.34}$$

and

$$\frac{-u\frac{\partial}{\partial u}(1/\zeta_\sigma(t,u))}{1/\zeta_\sigma(t,u)} = \sum_{n=1}^{\infty}\sum_{k=0}^{n-1}N_{n,k}u^n. \tag{D.35}$$

Using the product formula of this topological zeta function and the numbers of orbits with length up to 5 from the table **??**, the Kim-Lee-Park zeta function is:

$$1/\zeta_\sigma(t,u) = \sqrt{1-t^2}\exp\left(-\frac{u}{1-u}\right)(1-t^4)\exp\left(-\frac{2u^2}{1-u^2}\right)\left(\sqrt{1-t^6}\right)^3$$
$$\exp\left(-\frac{3u^3}{1-u^3}\right)(1-t^6)(1-t^8)^3\exp\left(-\frac{6u^4}{1-u^4}\right)$$
$$(1-t^8)^2(1-t^{10})^5\exp\left(-\frac{10u^5}{1-u^5}\right)(1-t^{10})^6\dots. \tag{D.36}$$

And the generating function from this topological zeta function is:

$$\frac{-u\frac{\partial}{\partial u}(1/\zeta_\sigma(t,u))}{1/\zeta_\sigma(t,u)} = u + 6u^2 + 12u^3 + 36u^4 + 55u^5 + \dots, \tag{D.37}$$

which is in agreement with (D.35), where the N_n^σ is the SF_n in the table **??**.

2021-12-10 Predrag

$$-\Box\, x_t + a\, x_t^2 - 2\, x_t - m_t \,=\, 0\,. \tag{D.38}$$

$$V(\Phi,\mathsf{M}) = \sum_{t\in\mathcal{L}}\left(\frac{g}{k}\phi_t^k - \phi_t^2 - m_t\,\phi_t\right), \qquad m_t = -1\,. \tag{D.39}$$

Works also for temporal cat:

$$V(\Phi, \mathsf{M}) = \sum_{t \in \mathcal{L}} \left(\frac{s}{2} \phi_t^2 - \phi_t^2 - m_t \, \phi_t \right) = \sum_{t \in \mathcal{L}} \left(\frac{s-2}{2} \phi_t^2 - m_t \, \phi_t \right) , \quad (D.40)$$

Appendix D.2. Hill determinant: fundamental parallelepiped evaluation

As a concrete example consider the Bravais lattice with basis vector
The *orbit Jacobian matrix* is the $\delta/\delta\phi_k$ derivative of the temporal Hénon three-term recurrence relation (**??**)

$$\mathcal{J}_p = \, -r + 2\,\mathbb{X}_p - r^{-1} \,, \qquad (D.41)$$

where $\mathbb{X}_p$ is a diagonal matrix with p-periodic state ϕ_k in the kth row/column, and the '1's in the upper right and lower left corners enforce the periodic boundary conditions.
The action of the temporal Hénon orbit Jacobian matrix can be hard to visualize, as a period-2 periodic state is a 2-torus, period-3 periodic state a 3-torus, etc.. Still, the fundamental parallelepiped for the period-2 and period-3 periodic states, should suffice to convey the idea. The fundamental parallelepiped basis vectors (**??**) are the columns of $\mathcal{J}$. The $[2\times2]$ orbit Jacobian matrix and its Hill determinant follow from (**??**)

$$\mathcal{J} = \begin{pmatrix} 2\,\phi_0 & -2 \\ -2 & 2\,\phi_1 \end{pmatrix} , \qquad \mathrm{Det}\,\mathcal{J} = 4\,(\phi_0\phi_1 - 1) = -4\,(a-3)\,. \quad (D.42)$$

The resulting fundamental parallelepiped shown in figure **??** (a). Period-3 periodic states for $s = 3$ are contained in the half-open fundamental parallelepiped of figure **??** (b), defined by the columns of $[3\times3]$ orbit Jacobian matrix

$$\mathcal{J} = \begin{pmatrix} 2\,\phi_0 & -1 & -1 \\ -1 & 2\,\phi_1 & -1 \\ -1 & -1 & 2\,\phi_2 \end{pmatrix} , \qquad \mathrm{Det}\,\mathcal{J} = 8\,\phi_0\phi_1\phi_2 - 2\,(\phi_0+\phi_2+\phi_3)+2\,, \quad (D.43)$$

2021-12-31 Han Note that in the temporal lattice reformulation, the Bernoulli system involves two distinct lattices:

(i) Any lattice field theory: in the discretization (1) of the time continuum, one replaces *any* dynamical system's time-dependent field $\phi(t) \in \mathbb{R}$ at time $t \in \mathbb{R}$ by a discrete set of its values $\phi_t = \phi(a\,t)$ at time instants $t \in \mathbb{Z}$. Here t is a *coordinate* over which the field ϕ is defined.

(ii) Specific to the Bernoulli system: the site t field value ϕ_t (**??**) is confined to the unit interval $[0, 1)$, imparting integer lattice structure onto the intermediate calculational steps in the extended state space (**??**) on which the orbit Jacobian matrix $\mathcal{J}$ (**??**) acts.

[2021-10-25 Predrag] Combine the above with the temporal cat page **??** discussion into a remark that temporal Bernoulli and temporal cat aslo have a *dynamical* D_1 symmetry, not utilized in this paper, as nonlinear field theories such as temporal Hénon do not have such symmetries. Here we study only the symmetries of the floor, not the dancer.

2020-05-31 Predrag Simó [190] *On the Hénon-Pomeau attractor* is a very fine early paper. Cite it in Hénon remark.

Miguel, Simó and Vieir [158] *From the Hénon conservative map to the Chirikov standard map for large parameter values* (click here):

Endler and Gallas [72]. method resembles the methods earlier employed for quadratic polynomials (and their Julia sets) by Brown [36] and Stephenson [195]. (PC 2022-01-03 now referred to.)

Brown gives cycles up to length 6 for the logistic map, employing symmetric functions of periodic points.

Hitzl and Zele [100] study the of the Hénon map for cycle lengths up to period 6.

2021-10-29 Predrag Dropped: , all five of form $\{\Phi_{m_0m_1m_2}, \Phi_{m_1m_2m_0}\Phi_{m_2m_0m_1}\}$.

2020-12-17 Predrag Gave up on linking temporal cat to ChaosBook, as Adler-Weiss partitions are not there yet. Maybe refer to Adler-Weiss in later version.

2021-12-28 Han Statement after refeq recipCircl is not correct. In the $k = 1$ and $k = n - 1$ subspaces, all reciprocal periodic states lie in complex plane on vertices of regular n-gons. Generally this is not true. See figures **??** and **??** $k = 2$ and $k = 3$ (in blogCat), where the shift r rotate the reciprocal periodic state by $2\pi/3$ and $2\pi/2$, instead of $2\pi/6$. I suggest we only mention $k = 1$ here.

2021-12-30 Predrag It does not say in The Bible that vertices of an n-gon have to be visited in increments of one. Periodic states lie on the vertices of n-gons for any k, they are just visited in different order for different k. An if n is not prime, some visitation sequences do not visit all vertices. That's OK. Every vertex is occupied.

2021-12-30 Predrag (**??**) formulas do not make sense to me for n odd...

$$\begin{aligned} N_n &= \left(\Lambda^{n/2} - \Lambda^{-n/2}\right)^2 , \\ N_{n,0} &= \Lambda^{n/2} - \Lambda^{-n/2} \end{aligned} \tag{D.44}$$

but I do remember all $\Lambda^{1/2}$ eventually going away... Never mind.

2021-12-30 Han For general s we have: $N_{n,0} = \sqrt{(s-2)N_n}$ (**??**). This is in agreement with table **??**.

2021-12-26 Han Given the symmetry group of the periodic states, we can find a fundamental domain in the space of field configurations such that each orbit in this space visits the fundamental domain only once. Each periodic state in the fundamental domain is a representative periodic state of an orbit.

A natural way to choose the fundamental domain of C_n symmetry group is to divide the subspace of a component of the reciprocal lattice configuration. In the subspace of the $k = 1$ Fourier mode, the fundamental domain is an $1/n$ wedge. The lattice shift r maps the fundamental domain by rotation and tiles the whole complex plane. Orbits visit the $1/n$ wedge only once, so the points in the fundamental domain represent an orbit each.

Repeats of the shorter periodic states sit on the 0 of the complex plane, which is on the boundary of the fundamental domain.

For example, one can choose the region in the complex plane of $\tilde{\phi}_1$ with argument $-\pi/2n \leq \theta_1 < \pi/2n$ to be the fundamental domain. Each orbit can visit the fundamental domain only once. For the period-3 periodic states of the temporal Bernoulli system with $s = 2$ shown in figure **??**, there are 3 points in this region, which are representative periodic states of two different period-3 orbits and the fixed point 0.

[2021-08-20 Predrag] Merge figure **??** (a) with *1dLatStatC_5_0x3.svg.*

2022-01-04 Han Moved from the end of section **??**

If, in addition, the law is time-reversal (or time-inversion) invariant, the symmetry includes time-reflection, ie, it is dihedral group D_n with $2n$ elements, so the reciprocal lattice should be a half of the above $1/n$ sliver of a n-gon, and irreps are now either 1 or 2 dimensional. Even n is different from odd n, and solutions either appear in pairs, or are self dual under reflection in 3 different ways.

Due to the time reversal, all $k = 2\pi/5$ irrep states are the same as the $k = 4\pi/5$ irrep states.

2022-01-15 Han where Φ and $\hat{f}(\Phi)$ are nd-dimensional column vectors with $(id+j)$th components $(\phi_t)_j$ and $[\hat{f}(\phi_t)]_j$, where $0 \leq i < n-1$, $0 \leq j < d-1$, and r is the cyclic $[nd\times nd]$ time translation operator (compare with (**??**), (**??**)):

$$r = \left(\begin{array}{cccccc} 0 & \mathbb{1}_d & & & & \\ & 0 & \mathbb{1}_d & & & \\ & & & \ddots & & \\ & & & & 0 & \mathbb{1}_d \\ \mathbb{1}_d & & & & & 0 \end{array}\right) , \tag{D.45}$$

where $\mathbb{1}$ is the d-dimensional identity matrix.

Just as a scalar field satisfying a kth order differential equation can be replaced by a k-component field, each satisfying a first order equation, a kth order difference equation for a scalar field can be replaced by a k-component lattice site field, satisfying k 1st order difference equations.

2022-01-16 Predrag Now I get it. To get from $\prod d^2\phi_t$ in (**??**) to $\prod d\phi_t$ in (**??**) we note that the first component of time-step (**??**) written in terms of 1-dimensional Dirac delta functions is trivial,

$$\begin{aligned} \int d\hat{\phi}_t\,\delta(\hat{\phi}_{t+1} - \hat{f}(\hat{\phi}_t)) &= \int d\hat{\phi}_{t,1} d\hat{\phi}_{t,2} \delta(\hat{\phi}_{t+1,1} - \hat{\phi}_{t,2}) \delta(\hat{\phi}_{t+1,2} - f(\hat{\phi}_{t,1}, \hat{\phi}_{t,2})) \\ &= \int d\hat{\phi}_{t,1} d\hat{\phi}_{t,2} \delta(\hat{\phi}_{t+1,1} - \hat{\phi}_{t,2}) \delta(\hat{\phi}_{t+2,1} - f(\hat{\phi}_{t,1}, \hat{\phi}_{t+1,1}) \\ &= \int d\hat{\phi}_{t,1} \delta(\hat{\phi}_{t+2,1} - f(\hat{\phi}_{t,1}, \hat{\phi}_{t+1,1}) \\ &= \int d\phi_{t-1} \delta(\phi_{t+1} - f(\phi_{t-1}, \phi_t)\,? \end{aligned} \tag{D.46}$$

where we have used periodicity and dropped the component subscript, $\hat{\phi}_{t,1} \to \phi_{t-1}$? Looking back: we should get rid of field component indices by using two Greek letters,
$\hat{\phi}_t = (\phi_t, \varphi_t)$, where $\varphi_t = \phi_{t+1}$.

2020-02-08 Predrag Gave up on this:
Complain about [92] Dirichlet bc's stupidity clearly both in the intro and in conclusions.

2022-01-17 Han I changed (**??**) from

$$\Delta\phi_t - r^{-1}\mathbb{J}_t\,\Delta\phi_t = 0$$

which is incorrect. The shift matrix r cannot act on the d-dimensional vector.
PC: OK.

2022-01-19 Predrag removed "If a potential that is bounded from below is needed to make sense of the probabilistic interpretation of the configuration weight (**??**)" from "one starts with a quartic potential (27) i.e., (64)" because our potential is inverted.
Dropped:
For the 1-dimensional temporal lattice examples studied here, the reader might not see much of an advantage in the global stability ('Lagrangian') formulation over the forward-in time stability ('Hamiltonian') formulation. The real payback is in the higher-dimensional spacetimes.
The fundamental fact does not apply to orbit counting for reversal-invariant nonlinear field theories, such as the temporal Hénon.
It is *prime* in the same sense that Leibnitz monad is indivisible.
Toeplitz, i.e., matrix constant along each diagonal, $\mathcal{J}_{k\ell} = j_{k-\ell}$.
For a finite set of neighbors, Allroth [5] has partial results in the context of Frenkel-Kontorova models.
we will spare the reader the group-theorist's cosets and group quotients.

2021-12-24 Predrag We have found MacKay [147] 1982 PhD thesis lists the periodic periodic states and orbits counts, together with the counts of time reversal invariant periodic states and orbits. Do cite in our paper(s). MacKay had these numbers already listed in Table 1.2.3.5.1 of his 1982 PhD thesis [147].

2022-01-22 Predrag Gave up on this confused insert on **Physical dimension**
Time evolution Jacobian matrices are nice, as to the their multiplicative structure (**??**), the Floquet matrix for the rth repeat of a prime period-n periodic state Φ_p (**??**) is known, once the prime periodic state Φ_p Floquet matrix (**??**) is known.
But that is actually quite meaningless, especially for infinite dimensional physical systems. What matters is the Hill determinant $|\mathrm{Det}\,\mathcal{J}_c| = |\det(\mathbb{1} - \mathbb{J}_c)|$, which is a finite number as long as there is a finite number of expanding directions; the contracting ones are only small corrections to 1.
If $\partial_i v_i < 0$ at a given state space point ϕ, the flow is *locally* contracting, and the trajectory might be falling into an attractor. If $\partial_i v_i(\phi) < 0$ for all $\phi \in \mathcal{M}$, the

flow is *globally* contracting, with the dimension of the attractor necessarily smaller than the dimension of state space $\mathcal{M}$. For ∞-dimensional dissipative flows, such as Navier-Stokes, the ∞ of stability multipliers Λ_i in can be arbitrarily small; as such exponents represent damping of arbitrarily kinky modes of a viscous fluid, they are of no interest for study of steady turbulence. So the product should be truncated to a finite number d_{phys} of leading stability exponents. We shall refer to this integer as a *physical* dimension of a *strange attractor*, in fluid dynamics often referred to as the *inertial manifold*. Every expanding or marginal direction contributes 1 to d_{phys}, and then to get a lower bound on d_{phys}, one has to keep at least as many contracting Λ_i as needed to ensure that the product is globally contracting. As nonlinear terms can mix various terms in such a way that expansion in some directions overwhelms the strongly contracting ones, d_{phys} is larger than this bound, but still a finite number.

This is an amazing result: a fluid's state space is ∞-dimensional, but its long term dynamics is confined to a finite-dimensional(!) subspace, the reason why we can apply the few degrees of freedom technology developed here to ∞-dimensional field theories.

2022-01-27 Predrag Uploaded LC21 [137] as `arXiv:2201.11325`.

For details, see `reversal/00ReadMe.txt`.

2022-01-30 Predrag Submitted LC21 [137] to *mc04.manuscriptcentral.com/jphysa-iop*

For referees, see *reversal/jphysa-v1/referees.txt*

2022-04-09 Predrag At the moment I do not remember the logic of labels in figure **??** (b) - good for desymmetrization? and why '6' rather than '0'?

2022-04-29 Han The subsection of D_∞ or Kim-Lee-Park zeta function needs to be rewritten.

If the assumed symmetry G is not the maximal symmetry group, let's say we assume only $G = \mathrm{C}_\infty$ whereas the full symmetry is D_∞, Lind zeta function (**??**) reduces to the Artin-Mazur zeta (**??**) which counts reflection symmetry-related periodic states as belonging to separate 'prime orbits', a problem that repeatedly bedevils the `ChaosBook.org` exposition of periodic orbit theory.

So our next task is to evaluate Lind zeta function when the symmetry group G of temporal lattice of a given dynamical system is the infinite dihedral group D_∞, the group of all translations and reflections, i.e., system's defining law is time and time-reversal invariant. For the infinite translation $H_\mathbf{a}$ subgroup (**??**) the index is (as illustrated by figure **??**)

$$|\mathrm{D}_\infty/H_n| = 2n\,. \tag{D.47}$$

As explained in section **??**, the D_∞ orbits of reflection-symmetric periodic states contain only translations, so the index of each infinite dihedral subgroup $H_{\mathbf{a},k}$ (**??**) is

$$|\mathrm{D}_\infty/H_{n,k}| = n\,. \tag{D.48}$$

Thus the state space $\mathcal{M}$ of a D_∞ invariant dynamical system is the union

$$\mathcal{M} = \mathcal{M}_a \cup \mathcal{M}_s\,, \tag{D.49}$$

where $\mathcal{M}_a$ is the set of pairs of asymmetric orbits (**??**), each element of the set a forward-in-time orbit and the time-reversed orbit, and $\mathcal{M}_s$ is the set of time reversal symmetric orbits, invariant under reflections (**??**–**??**).
The Lind zeta function (**??**) now has contributions from asymmetric periodic states, whose index is (D.47), and symmetric periodic states, index (D.48):

$$\zeta_{\mathrm{D}_\infty}(t) = \exp\Big(\sum_{n=1}^{\infty}\frac{N_n}{2}\frac{t^{2n}}{n} + \sum_{n=1}^{\infty} N^s_n\frac{t^n}{n}\Big)\,. \tag{D.50}$$

$N_n/2$ counts each asymmetric orbit pair of period n only once, so the first sum yields the Artin-Mazur zeta function $\zeta_{\mathrm{a}}(t^2)$ for the asymmetric periodic states:

$$\zeta_{\mathrm{D}_\infty}(t) = \zeta_{\mathrm{a}}(t^2)\,\zeta_{\mathrm{s}}(t)\,. \tag{D.51}$$

In order to count the symmetric periodic states, we have to take into account the fact that the three types of symmetric periodic states of section **??** have to be counted separately, as their orbit Jacobian matrices satisfy different boundary conditions,

$$\zeta_{\mathrm{s}}(t) = \exp\Big(\sum_{n=1}^{\infty}\sum_{k=0}^{n-1}\frac{N^s_{n,k}}{n}t^n\Big)\,. \tag{D.52}$$

The number of reflection-symmetric periodic states does not depend on the location of the reflection point k, only on the type of symmetry (see the class counts (**??**) and (**??**)), so

$$N^s_{n,k} = \begin{cases} N^s_{n,0} & \text{if } n \text{ odd} \\ N^s_{n,0} & \text{if } n \text{ and } k \text{ are even} \\ N^s_{n,1} & \text{if } n \text{ even and } k \text{ is odd}\,, \end{cases} \tag{D.53}$$

and the Lind zeta function takes the form that we refer to as the Kim-Lee-Park [128] zeta function

$$\zeta_{\mathrm{D}_\infty}(t) = \zeta_{\mathrm{a}}(t^2)\,e^{h(t)}, \tag{D.54}$$

where

$$h(t) = \sum_{m=1}^{\infty}\Big\{N^s_{2m-1,0}\,t^{2m-1} + \big(N^s_{2m,0}+N^s_{2m,1}\big)\,\frac{t^{2m}}{2}\Big\}\,. \tag{D.55}$$

Appendix D.2.1. Euler product form of Kim-Lee-Park zeta function. Kim *et al* [128] show that the contribution of a single prime orbit p to the Kim-Lee-Park zeta function is:

$$1/\zeta_{\mathrm{D}_\infty}(t)|_p = \begin{cases} 1 - t^{n_p} & \text{if } p \in \mathcal{M}_a\,, \\ \sqrt{1-t^{2n_p}}\,\exp\big(-\frac{t^{n_p}}{1-t^{n_p}}\big) & \text{if } p \in \mathcal{M}_s\,, \end{cases} \tag{D.56}$$

with the zeta function written as a product over prime orbits:

$$1/\zeta_{\mathrm{D}_\infty}(t) = \prod_{p_a \in \mathcal{M}_a} (1 - t^{n_{p_a}}) \prod_{p_s \in \mathcal{M}_s} \sqrt{1 - t^{2n_{p_s}}} \exp\left(-\frac{t^{n_{p_s}}}{1 - t^{n_{p_s}}}\right) , \quad \text{(D.57)}$$

to be expanded as a power series in t.

The Euler product form of topological zeta functions makes it explicit that they count *prime orbits*, i.e., sets of equivalent periodic states related by symmetries of the problem. The remainder of this section the reader might prefer to skip: we verify by explicit temporal cat calulation that the Kim-Lee-Park zeta function indeed counts infinite dihedral group D_∞ orbits and the corresponding periodic states.

2022-05-02 Predrag to Angelo Vulpiani

Long silence because I have not YET (!) started reading Il Libro [39] (click here). Grazie for sharing it, and I'll get to it eventually, but... The usual physicist obsession – we had run into a wall exploring "exact coherent structures" in fluid dynamics, and my resolution is to take the revolutionary road: kill dynamical systems and retreat to field theory/stat mech. It has been very hard to write it up in a way that gets it across – here is part of it (with video clips)
https://chaosbook.org/overheads/spatiotemporal/LC21.pdf
And much talking about it over last few years:
https://chaosbook.org/overheads/spatiotemporal/
I think it might align with some of your work way back then, tell me if I should read/cite something in particular.

Note to Han & Predrag send
`https://chaosbook.org/overheads/spatiotemporal/LC21.pdf`
link to
Michael Aizenman
(R. E. Amritkar and gade are not active)
S. Anastassiou
Ping Ao aoping@sjtu.edu.cn
Roberto Artuso artuso@fis.unico.it
Serge Aubry
Erik Aurell eaurell@kth.se
Bountis
Dwight Barkley d.barkley@warwick.ac.uk University of Warwick
A. Bäcker
A. Barvinok
David Berenstein ¡dberens@physics.ucsb.edu¿
Ofer Biham
Erik M. Bollt ebollt@clarkson.edu Clarkson University

S. V. Bolotin
A. Bountis
H. Chat'e
Xiangyu Cao ¡xiangyu.cao08@gmail.com¿
B. Clair
A. M. Ozorio de Almeida
Carl Dettmann
H. R. Dullin
Marco Falconi marco.falconi@polimi.it
Farazmand
Jason Gallas
Gutkin
Jonathan Halcrow
Masanori Hanada ¡hanadamasanori@gmail.com¿
J. H. Hannay
S. Isola
W. Just
Jon Keating j.p.keating@bristol.ac.uk University of Bristol
J. Li
Douglas Lind
R. S. MacKay
Ronnie Mainieri
James Meiss jdm@colorado.edu University of Colorado
Kevin Mitchell kmitchell@ucmerced.edu University of California Merced
I. Montvay
G. Münster
E. Ott
Kyewon Koh Park kkpark@kias.re.kr Korea Inst. Adv. Study
Antonio Politi a.politi@abdn.ac.uk U Aberdeen
M. Pollicott
C. Pozrikidis
Tomaz Prosen tomaz.prosen@fmf.uni-lj.si University of Ljubljana
Putkaradze
Klaus Richter klaus.richter@physik.uni-regensburg.de Universität Regensburg
Martin Richter ¡martin.richter@nottingham.ac.uk¿
Ruelle
S. Saito
Marcos Saraceno saraceno@tandar.cnea.gov.ar CNEA-GIyA Laboratorio Tandar
George Savvidy, "Demokritos", Athens
(the other two not active? Young-One Kim, Jungseob Lee)
Tobias Schneider
Michele Schiavina (ETH Zürich

Steve Shenker
David G. Sterling dsterling@somalogic.com (old?)
T. Sunada
G. Tanner
Jean-Luc Thiffeault jeanlucth@gmail.com 2022-05-02
S. Tomsovic
Alessandro Torcini ¡alessandro.torcini@u-cergy.fr¿
D. V. Treschev
Tuckermann
Gabor Vattay
Divakar Viswanath divakar@umich.edu University of Michigan
Franco Vivaldi f.vivaldi@qmul.ac.uk Queen Mary University of London
Angelo Vulpiani angelo.vulpiani@roma1.infn.it 2022-05-02
Wiegmann
Ashley Willis

Contacted
Vladimir Rosenhaus ¡vrosenhaus@gc.cuny.edu¿
Baladi
Rafael De La Llave

Appendix E. Integer lattices literature

There are many reasons why one needs to compute an “orbit Jacobian matrix” Hill determinant $|\mathrm{Det}\,\mathcal{J}|$, in fields ranging from number theory to engineering, and many methods to accomplish that:

discretizations of Helmholtz [60, 78, 139] and screened Poisson or Klein–Gordon or Yukawa [61, 89, 108, 109] equations

Green’s functions on integer lattices [8, 10, 26, 37, 40, 45, 79, 87, 105, 106, 123–125, 144, 152, 154, 161, 162, 172, 199, 217]

linearized Hartree-Fock equation on finite lattices [127]

random walks, resistor networks, electrical circuits [4, 11, 28, 51, 52, 62, 90, 94, 111, 129, 133, 166, 177, 201, 206, 219]

Gaussian model [83, 120, 151, 188]

tight-binding Hamiltonians [51, 52, 69]

discrete Schrödinger equation [171], Harper or Hofstadter model [96, 104] or almost Mathieu operator [191]

quasilattices [34, 82]

circulant tensor systems [37, 40, 157, 178, 182, 221]

Ising model [20, 101, 102, 110, 112, 114–116, 126, 138, 146, 153, 167, 173, 220], Ising model transfer matrices [168, 220]

lattice field theory [118, 155, 160, 164, 185, 192, 193, 211]

many-body quantum chaos [1–3, 22–25, 73–77, 183]

modular transformations [38, 132, 225]

lattice string theory [86, 169]

spatiotemporal stability in coupled map lattices [6, 85, 223]

Van Vleck determinant, Laplace operator spectrum, semiclassical Gaussian path integrals [135, 136, 205, 207]

Jacobi operator

time reversal

Hill determinant [29, 148, 207]; discrete Hill's formula and the Hill discriminant, Toda lattice [204]

Lindstedt-Poincaré technique [208–210]

heat kernel [41, 65, 70, 119, 122, 154, 172, 222]

chronotopic models [175]

lattice points enumeration [17, 18, 21, 57]

cryptography [156]

primitive parallelogram [14, 35, 165, 212]

difference equations [56, 80, 200]

Bernoulli map [33, 64, 103], beta transformation [81, 170, 181]

digital signal processing [66, 140, 218]

generating functions, Z-transforms [70, 214]

integer-point transform [21]

graph Laplacians [46, 88, 143, 176]

graph zeta functions [9, 16, 19, 32, 47–49, 58, 65, 91, 97, 107, 113, 131, 134, 176, 180, 186, 187, 194, 202, 203, 224]

zeta functions for multi-dimensional shifts [15, 141, 142, 159]

zeta functions on discrete tori [41, 42, 222]

Appendix F. Nonlinear deterministic field theory WWLAFC22blog

The latest entry at the bottom of this section, page 68

Internal discussions of [215]: we saved text not used in [215] here, for possible reuse in [55], or elsewhere.

2022-04-03 Predrag the initial version of rescaling, from **2022-03-14**. Leads to a pesky parameter $\mu^2/2$, superseded by section 7 *Deterministic ϕ^3 lattice field theory*:

$$V_1(\phi) = -\frac{g}{3!}\phi^3 + \frac{\mu^2}{2}\phi^2 = -\frac{g}{3!}\left(\phi^3 - 3\lambda\,\phi^2\right), \quad \lambda = \mu^2/g\,, \tag{F.1}$$

$$f(x) = x^3 + p\,x\,, \tag{F.2}$$

field translation $\phi \to \phi + \epsilon$:

$$-\frac{g}{3!}\Big((\phi+\epsilon)^3 - 3\lambda(\phi+\epsilon)^2\Big) = -\frac{g}{3!}\Big(\phi^3 + 3(\epsilon-\lambda)\phi^2 + 3\epsilon(\epsilon-2\lambda)\phi\Big) + (\mathrm{const})\,.$$

field translation $\epsilon = \lambda$, such that the ϕ^2 term vanishes,

$$V_1(\phi) = -\frac{g}{3!}(\phi^3 - 3\lambda^2\phi) + (\mathrm{const})\,.$$

Rescale the field $\phi \to \lambda\,\phi$, and drop the (const) term:

$$V_1(\phi) = -\frac{g}{3!}\phi^3 + \frac{\mu^2}{2}\phi \to -\lambda^2\frac{\mu^2}{3!}\,(\phi^3 - 3\phi)\,.$$

$$S[\Phi] = \frac{\mu^4}{g^2}\sum_z \Big\{ -\frac{1}{2}\phi_z\Box\phi_z - \frac{\mu^2}{3!}\,(\phi_z^3 - 3\phi_z)\Big\}\,. \tag{F.3}$$

$$-\phi_{t+1} + 2\,\phi_t - \phi_{t-1} - \frac{\mu^2}{2}\,\phi_t^2 + \frac{\mu^2}{2} \;=\; 0\,, \tag{F.4}$$

Period-1 periodic states.

$$F[\overline{\phi}] = \frac{\mu^2}{2}(1-\phi_t^2)\,, \tag{F.5}$$

with two real roots $\overline{\phi}_m$

$$(\overline{\phi}_L, \overline{\phi}_R) = (-1, 1)\,. \tag{F.6}$$

Period-2 periodic states. (Never crosschecked)

four period-2 periodic states $\overline{\Phi}_m = \overline{\phi_0\phi_1}$, set $x = \phi_{2k}$, $y = \phi_{2k+1}$ in the Euler–Lagrange equation (F.4), and seek the zeros of

$$F[x,y] = \begin{pmatrix} 2(x-y) - \frac{\mu^2}{2}(x^2-1) \\ 2(y-x) - \frac{\mu^2}{2}(y^2-1) \end{pmatrix}. \tag{F.7}$$

$$F_2[x, y(x)] = \frac{\mu^4}{16}(x-1)(x+1)\Big(x^2 - (1 - \frac{8}{\mu^2})\Big) \tag{F.8}$$

symmetric period-2 periodic state $\overline{\underline{1}2}$

$$x = -y = \pm\sqrt{1 - 8/\mu^2}\,, \tag{F.9}$$

prime period-2 periodic state exists for $\mu > 8$.

2024-03-06 Predrag

$$\mathcal{J}_H = \begin{pmatrix} 2a\gamma_0 & -1 & 0 & 0 & \cdots & 0 & -1 \\ -1 & 2a\gamma_1 & -1 & 0 & \cdots & 0 & 0 \\ 0 & -1 & 2a\gamma_2 & -1 & \cdots & 0 & 0 \\ \vdots & \vdots & \vdots & \vdots & \ddots & \vdots & \vdots \\ 0 & 0 & 0 & 0 & \cdots & 2a\gamma_{n-2} & -1 \\ -1 & 0 & 0 & 0 & \cdots & -1 & 2a\gamma_{n-1} \end{pmatrix} \tag{F.10}$$